PHOTOCATALYTIC REDUCTION OF TRACE AQUEOUS MERCURY USING A VISIBLE LIGHT SOURCE

By

ERICA WALLACE GONZAGA

A THESIS PRESENTED TO THE GRADUATE SCHOOL
OF THE UNIVERSITY OF FLORIDA IN PARTIAL FULFILLMENT
OF THE REQUIREMENTS FOR THE DEGREE OF
MASTER OF ENGINEERING

UNIVERSITY OF FLORIDA

2014

To my family

ACKNOWLEDGMENTS

I would like to thank my advisor, Dr. David Mazyck, for opening the doors to research and offering an opportunity to work with his graduate students when I will still completing my undergraduate degree. I am also grateful for the guidance he has offered in the past two years of graduate school. I would like to thank Dr. Jean-Claude Bonzongo, Dr. Paul Chadik and Dr. Wolfgang Sigmund for serving on my committee.

I am grateful for the wonderful research team and colleagues that have helped me throughout graduate school: Christine Valcarce, Amy Borello, Sanaa Jaman and Ana Maria Hagan. Thank you to all CCI employees, especially Regina Rodriguez, for offering assistance whenever I needed it. I am grateful for the help and hard work of my undergraduate assistant Sutanya Singivipulya.

Lastly, I would like to thank my husband Luiz Gonzaga for being patient and understanding. You have been the most supportive partner I could ask for and I am grateful for having you in my life.

TABLE OF CONTENTS

LIST OF TABLES

LIST OF FIGURES

Abstract of Thesis Presented to the Graduate School
of the University of Florida in Partial Fulfillment of the
Requirements for the Degree of Master of Engineering

PHOTOCATALYTIC REDUCTION OF TRACE AQUEOUS MERCURY USING A VISIBLE LIGHT SOURCE

By

Erica Wallace Gonzaga

May 2014

Chair: David Mazyck
Major: Environmental Engineering Sciences

Mercury emissions may originate from both natural and anthropogenic sources. As regulations become stricter, refined removal processes may be required to reduce trace concentrations. The photocatalytic properties of semi-conducting materials have been investigated extensively using ultra-violet (UV) light, but high costs associated with UV energy make photocatalysis an impractical treatment method. Studies were conducted to investigate the potential of using photocatalysis for the reduction of trace aqueous mercury using a visible light source.

A silica-titania composite (STC) was mixed with tungsten oxide (WO_3) to determine if co-mixing semi-conductors may improve the photocatalytic potential. Removal of mercury increased slightly in the co-mixing studies compared to single catalysts, but it was determined that enhanced adsorption and not photocatalytic reduction contributed to better removal. However, positive results from STC experiments using visible light lead to further investigation of its photocatalytic potential. Experiments were conducted to understand the effect of contact time, catalyst dose, dissolved oxygen and the presence of an organic oxygen scavenging compound (formic acid) using STC and TiO_2. More than 95% removal was achieved within 15 minutes

using STC when formic acid and/or a nitrogen purge were utilized. Detailed 5 minute experiments demonstrated that the presence of formic acid is the most important factor affecting removal; acting as a radical a scavenger and preventing re-oxidation of mercury. With formic acid present, reduction of mercury ranged between 82-98% for different STC concentrations. The presence of dissolved oxygen affected removal negatively only when formic acid was used; reducing removal by approximately 40%.

Lastly, the effect of initial concentration of mercury was investigated. Visible light was effective at photoreducing mercury by more than 80% at low concentrations of 50 and 100 parts per billion using STC. There was no statistical difference between removals with visible light compared to UV 254 nm at these concentrations. However, removal rates decreased drastically as mercury concentrations increased to 500 and 1000 ppb as hypothesized. At 1000 ppb, mercury removal was only about 15% using visible light compared to more than 95% using UV 254 nm. The reduction of mercury is directly proportion to available electrons from the photocatalyst.

CHAPTER 1
INTRODUCTION

Opening Statement

The toxicity of mercury was first recognized in the early 1950s when a chemical plant discharged an estimated 70-150 tons of inorganic mercury into Minamata Bay in Japan. The fish in the bay displayed mercury concentrations of approximately 15 ppm [1]. The local residents relied heavily on the consumption of fish and started developing methylmercury poisoning symptoms. Some of these symptoms included impairment of speech, muscle weakness, vision problems and numbness of hands and feet [2].

Awareness about the toxicity of mercury has increased since the 1950s and countries all around the world are working on implementing mercury emission regulations. In the United States, the regulatory limit of mercury in drinking water is 0.002 mg/L; a concentration believed to not affect human health [3]. In 2013, an international treaty known as Minamata Convention was signed by 140 countries, including the United States, pledging to regulate and reduce mercury emissions [4].

Photocatalytic treatment of heavy metals has been gaining more attention from the scientific community in the past couple of decades. Unlike other treatment process such as precipitation and adsorption, photocatalytic oxidation/reduction is capable of reducing contaminants to trace or nearly undetectable levels. When a catalyst is exposed to ultra-violet light, the photon energy excites an electron from the valence band causing it to jump to the conduction band. This is known as the electron-hole pair. This pair is responsible for generating redox reactions if recombination of the electron does not occur.

Many studies have focused on the modification of a photocatalyst, such as titanium dioxide (TiO_2), for use of visible light. Most of these studies have characterized the catalyst, measuring light absorbance/reflectance and binding energy, but there has not been substantial research on applying these modified catalysts in treatment processes. It has been noted that mercury has been reduced in natural systems exposed to sunlight, which contains less than 5% UV rays [5]. Other studies have questioned whether just a small percentage of UV photons are necessary to induce photocatalytic reactions.

The purpose of this study herein is to investigate the potential of photocatalytic reduction of trace aqueous mercury under visible light. Since most modification techniques include doping the catalyst with another metal, the effect of co-mixing catalysts (two semi-conductor metals) will be investigated.

Most other studies have tested visible light catalysis with high concentration of contaminants (ppm range). If the formation of electron-hole pairs is directly proportional to the intensity of light, and the reduction of mercury depends on the number of electron-hole pairs, then it is hypothesized that visible light (which emits low levels of UV light) may be effective at reducing low concentrations of mercury (ppb range).

Objectives

Investigate the potential of using co-mixed catalysts in the photocatalytic reduction of aqueous mercury under visible light.

Optimize the visible light photocatalytic process using a silica-titania composite by controlling dissolved oxygen, organic concentration and catalyst concentration.

Compare the performance of titania immobilized with silica to conventional titanium dioxide exposed to visible light.

Investigate the effects of initial concentration of mercury on visible light photocatalysis.

CHAPTER 2
LITERATURE REVIEW

Mercury

Mercury is present naturally in the environment and exits in three different forms that vary in toxicity: elemental, organic, and inorganic. The elemental form of mercury is released into the environment naturally through erosion and volcanic eruptions but anthropogenic sources are responsible for approximately 70% of mercury (Hg) released today [6]. Its toxic nature was discovered in the mid 1900's and laws regulating emissions are still debated today.

Sources

Most of the mercury transport in the atmosphere originates from anthropogenic sources. The main industrial activities that contribute to emissions include gold mining, pharmaceutical production, manufacturing of light bulbs and thermometers, metal processing and chlor-alkali chlorine production facilities among others. By far, the largest source of anthropogenic Hg emissions is coal-fired power plants, accounting for close to 50% of industrial discharges [6] [7].

The combustion of coal is responsible for the emission of both elemental and oxidized forms of mercury. Divalent Hg^{2+} is highly reactive and has a lifetime in the atmosphere of only a few days. It is deposited on land or in water close to its point of emission. Once deposited, oxidized mercury has the potential to transform into methylmerucy; a highly toxic, organic form of mercury. On the other hand, elemental mercury has a lifetime in the atmosphere of approximately one year and can travel long distances, contaminating areas far from the point of emission.

In the United States, mercury concentration in coal ranges from 0.8 to 1 μg/g [7]. During combustion, mercury is released from coal as its gaseous, elemental form. The total concentration of mercury in flue gas emissions ranges from 1 to 35 μg/N m^3 [8]. As the flue gas cools, part of the gaseous mercury gets oxidized to HgO, $HgCl_2$ or Hg_2Cl_2. Wet scrubbers or dry sorbent injection are common treatment processes used to remove the oxidized mercury. If not captured or treated, the remaining 50% of elemental mercury gets released to the atmosphere.

Contamination of water can occur via atmospheric transport or direct industrial discharge. Mercury emitted hundreds, or even thousands, of miles away can be discharged to the soil or a body of water through rainfall, thus contaminating drinking water sources. Elemental mercury released into the environment can get oxidized by ozone in the atmosphere to its divalent form from where it can be returned to the surface of the Earth through wet or dry deposition [9]. Once deposited, it may bind with other compounds on the surface or is re-emitted to the atmosphere as gaseous mercury.

Regulations

In the United States, mercury emissions are currently regulated by the Environmental Protection Agency (EPA) under the Safe Drinking Water Act (SDWA), the Clean Water Act (CWA), the Clean Air Act (CAA), and the Resource Conservation and Recovery Act (RCRA).

In 2005, the EPA created the Clean Air Mercury Rule under the CAA with the intention of reducing emissions for coal-fired power plants by setting caps. The rule was voided in 2009 when the D.C. Circuit removed power plants from the list of hazardous contaminant sources of the CAA [10]. In 2012, the EPA issued the Mercury and Air

Toxic Standards (MATS) with the intention of reducing air pollutants for oil and coal-fired power plants. The proposed rules will regulate emissions from plants generating 25 megawatts or more and allows each plant up to 4 years to comply with the technology-based standards [11].

In 1992, the EPA issued the Impaired Waters and Total Maximum Daily Load (TMDL) Regulations which limits the amount of contaminants that may be discharged into a body of water. Point source discharges are controlled by the National Pollutant Discharge Elimination System (NPDES) in which permits are issued by individual states [12]; therefore the TMDL for mercury varies from state-to-state. The drinking water in the United States is protected by the SDWA, which was passed in 1974 [3]. It sets standards and ensures the quality of municipal drinking water around the country. The regulation of mercury under the SDWA began in 1992 and the maximum contaminant level (MCL) in drinking water is 0.002 mg/L or 2 ppb [3].

In 2013, the Minamata Convention on Mercury was created to reduce anthropogenic emissions of mercury around the globe. A 2001 global assessment of mercury conducted by the United Nations Environmental Programme (UNEP) provided sufficient evidence on the negative impacts of mercury. Negotiations started in 2009 and after 4 years the treaty was finalized and signed by over 140 countries including the United States [4].

Health Impacts

Exposure to mercury can occur via inhalation, ingestion, or through dermal contact. Mercury may exist as a cation which gives it the potential to react with most ligands in living cells. Elemental mercury (Hg^0) is the least toxic species of the heavy

metal. If ingested, it is a stable, unreactive element in the body that will pass through the digestive system and be eliminated without causing harm.

In bodies of water, mercury undergoes biomethylation by specific organisms to form one of the most toxic species known as methylmercury (MeHg) [13]. It is suggested that methylmercury reacts with cysteine to form a compound that mimics the essential amino acid methionine [14]. Methionine is capable of entering the brain barrier and is always the first amino acid to start the polypeptide chain [14]. Therefore, when methylmercury enters the body, it is capable of penetrating the brain and inhibiting protein synthesis.

MeHg is ingested by fish and other aquatic organisms which in turn are consumed by humans. Mercury binds to proteins and lipids and can cause serious harm to the brain and nervous system. In adults, mercury contamination may cause headaches, nausea, vomiting, numbness, and difficulty walking, seeing, speaking and hearing among other symptoms [15]. Fetuses and young children are more susceptible to the damaging effects of mercury and exposure may cause a series of developmental issues including cerebral palsy, retardation and seizures [16].

The toxicity of MeHg was not recognized until the 1950s when the population of Minamata, Japan began developing serious neurological problems. Contamination of the water occurred via wastewater discharge from a Chisso Corporation plant that manufactured fertilizers [17]. The local population relied heavily on the contaminated fish as their source of protein. Adults developed serious symptoms affecting the neurological system, similar to epilepsy, known as Minamata disease. 30 cases of

cerebral palsy were reported due to mothers who consumed the contaminated fish during pregnancy [18].

Chemistry

Mercury is a heavy metal that exists in three oxidation states, Hg^0, Hg^+, and Hg^{2+}. Gaseous mercury in the atmosphere exists primarily in its elemental state, Hg^0. The divalent form is found in dissolved waters or attached to particles [19]. Therefore the oxidized form of mercury, Hg^{2+}, tends to be discharged from the atmosphere through precipitation, close to its source of emission [20]. On the other hand, Hg^0 is less soluble and will travel long distances across the globe before it is oxidized and released back to the earth. The lifetime of Hg^0 in the atmosphere could last up to 2 years [20].

Across varying pH values and chloride concentrations, the divalent form of mercury will complex with hydroxide and chloride ions in surface waters with an oxic environment. Hg will complex with hydroxide ions at pH values greater than 3 or when there is no chloride present and will hydrolyze to $HgOH^+$ and $Hg(OH)_2$ according to Equations (2-1and (2-2 [21].

$$Hg^{2+} + H_2O \rightleftarrows HgOH^+ + H^+ \quad (2\text{-}1)$$

$$HgOH^+ + H_2O \rightleftarrows Hg(OH)_2 + H^+ \quad (2\text{-}2)$$

$HgOH^+$ is predominant in the lower pH range of 2.2 to 3.8 while $Hg(OH)_2$ occurs at pH above 3.8 and being the only hydrolyzed species at pH 6 and above. Examining the various hydrolyzed species of mercury suggests the degree of solubility of the heavy metal. At natural water pH ranges, mercury will be present as a soluble hydrolyzed complex rather than free ions.

However, divalent mercury has a large affinity for complexation with chloride rather than hydroxide in oxic environments. At lower pH values, the Hg-Cl complexation

will form four species depending on the concentration of Cl^- present in solution: $HgCl^+$, $HgCl_2$, $HgCl^-_3$, and $HgCl^{2-}_4$ [22] where $HgCl_2$ is the predominant species. An intermediate species, HgClOH may be formed with in a small window of precise pH and chloride concentration values.

As discussed in subsequent sections, $Hg(NO_3)_2$ was used in this study. The compound ionizes into NO_3^- and Hg^{2+}. Since no other ions are present in solution, the mercury ions will hydrolyze as seen in Figure 2-1 [23].

Photocatalysis

Photocatalytic oxidation has been widely used for the treatment of organic compounds in water and air streams. In the past 20 years, interest has been increasingly shifting to the potential of using photocatalysis in the reduction of heavy metals from aqueous waste streams. Many metal oxides display photocatalytic properties. These semiconductors contain a void area, where no energy levels are available, known as the band gap [24]. When the semiconductor is exposed to light at a specific wavelength, an electron jumps the band gap from the valence band to the conduction band producing a positively charged hole (h^+) in the valence band and a photoexcited electron (e^-) in the conduction band. This is known as an electron-hole pair (Equation (2-3) [25]. The amount of energy required to produce an electron-hole pair must be equal to or greater than the band gap energy, in most cases UV or near UV light is required [24]. Recombination of the electron to the valence band can occur almost instantaneously if no other reactions take place. Instead of recombination, the electron-hole pair may participate in redox reactions with molecules adsorbed to the surface of the catalyst. The positively charged hole becomes available to oxidize any

nearby compounds while the negatively charged conduction band promotes a reduction reaction.

Oxidation Reactions

Valence band holes may directly oxidize a target pollutant or create hydroxyl radicals in the water. Hydroxyl radicals are believed to be the primary oxidants in photocatalytic oxidation and may be produced through various mechanisms. Water molecules adsorbed by the catalyst or OH^- groups on the surface of the catalyst may interact with the valence band to produce hydroxyl radicals as described by Equations (2-4 and (2-5 [26] [27] [28].

$$TiO_2 \overset{h\nu}{\rightarrow} \quad h_{vb}^+ + e_{cb}^- \tag{2-3}$$

$$H_2O + \ h_{vb}^+ \rightarrow \cdot OH + H^+ \tag{2-4}$$

$$OH^- + h_{vb}^+ \rightarrow \cdot OH \tag{2-5}$$

It is also suggested that hydroxyl radicals may be formed by the interacting of oxygen with the conduction band electron to form a superoxide ion which then transforms into hydrogen peroxide as described by Equations (2-6 through (2-10 [29]. The hydrogen peroxide molecules are then broken into hydroxyl radicals by interaction with the conduction band electron, by reacting with the superoxide ion or by direct photolysis (Equations (2-11 through (2-13) [28] [30] [31].

$$O_2 + e_{cb}^- \rightarrow \ O_2^{\cdot -} \tag{2-6}$$

$$O_2^{\cdot -} + H^+ \rightarrow HO_2 \cdot \tag{2-7}$$

$$HO_2 \cdot + HO_2 \cdot \rightarrow H_2O_2 + O_2 \tag{2-8}$$

$$O_2^{\cdot -} + \ HO_2 \cdot \rightarrow HO_2^- + O_2 \tag{2-9}$$

$$HO_2^- + H^+ \rightarrow H_2O_2 \tag{2-10}$$

$$H_2O_2 + e_{cb}^- \rightarrow \cdot OH + OH^- \quad (2\text{-}11)$$

$$H_2O_2 + O_2^{\cdot -} \rightarrow \cdot OH + OH^- + O_2 \quad (2\text{-}12)$$

$$H_2O_2 \xrightarrow{h\nu} 2 \cdot OH \quad (2\text{-}13)$$

Reduction Reactions

Many studies have focused on the photooxidation of organic contaminants, but slowly there has been an attention shift to investigating the photoreduction of heavy metals and inorganic compounds [32].

For photoreduction to be thermodynamically achievable, the reduction potential of the metal ion must greater than the energy of the conduction band of the photocatalyst [33] [34] . The size of the gap between the conduction (cb) and valence (vb) bands will remain constant, but the energy levels will alter with a change in pH. The difference in energy levels is quantified by Equations (2-14 and (2-15 [35] [36].

$$E_{cb} = (-0.05 - 0.059pH)\ eV \quad (2\text{-}14)$$

$$E_{vb} = (3.25 - 0.059pH)\ eV \quad (2\text{-}15)$$

According to the equations above, the photoreduction of mercury should increase with an increasing pH. It has been discussed that the photoreduction of a metal ion is directly proportional to the adsorption of the metal on to the surface of the photocatalyst [37]; therefore increasing the amount of metal ions adsorbed should increase the rate of photoreduction. However, an increased in absorbed metal ions increases the chances of photooxidation by the valence band hole [34] [38].

The following products are produced through the photocatalytic reductions of varying mercury salts in neutral or acidic pH (Equations 2-16 through 2-18) [39]:

$$Hg(NO_3)_2 + H_2O \rightarrow Hg^0 + \frac{1}{2}O_2 + 2HNO_3 \quad (2\text{-}16)$$

$$4HgCl_2 + 2H_2O \rightarrow 2Hg_2Cl_2 + O_2 + 4HCl \rightarrow 4Hg^0 \quad (2\text{-}17)$$

$$Hg(ClO_4)_2 + H_2O \rightarrow Hg^0 + \frac{1}{2}O_2 + 2HClO_4 \quad (2\text{-}18)$$

At a high pH, elemental mercury is oxidized according to Equation 2-19 [39]:

$$Hg^0 + O_2 \rightarrow HgO \quad (2\text{-}19)$$

The reduced form of mercury may be eliminated from the system through volatilization or removed through adsorption on to the catalysts.

Creating a Reducing Environment

Treatment techniques may be tailored to favor oxidation or reduction reactions. A reducing environment is preferable when treating aqueous mercury. Organic materials may be added to act as a hole scavenger and/or radical sink. In the presence of nitrogen purge, formic acid displayed the highest amount of carbon oxidized compared to acetic acid, methanol, ethanol, sucrose, and salicylic acid; oxidizing twice as much carbon as acetic acid at the 40 minute interval [40].

Formic acid is a small molecule that can be adsorbed on to the surface of TiO_2 impeding recombination by interaction with the valence band hole to produce carbon dioxide and water through the oxidation reaction. It will absorb only high energy light at wavelengths less than 260 nm [34] which means that formic acid will not be in competition with TiO_2 for the absorbance of lower energy UVA rays. These advantages make formic acid a suitable hole scavenger in the photoreduction of mercury as seen by Wang et al where the addition greatly increased the amount of mercury photoreduced [34]. However, it is important to note that the amount of formic acid necessary is directly proportional to number of electrons necessary for reduction. In a study investigating the

enhanced photocatalytic reduction of nitrate over Bi-doped TiO_2, it was noted that 5 moles of electrons are required to completely reduce 1 mole of nitrate to nitrogen gas [41]. Therefore, 5 moles of formic acid would be necessary. In the case of mercury reduction, two electrons are required for the formation of elemental mercury requiring two moles of formic acid per mole of mercury as seen in Equation 2-20:

$$Hg^{2+} + 2e^{-} \rightarrow Hg^{0} \qquad (2\text{-}20)$$

This is consistent with the results obtained by Wang et al; the addition of formic acid at concentrations more than double the concentration of mercury showed no improved photoreduction [34].

As covered earlier, the presence of dissolved oxygen may hinder the reduction of heavy metals. Oxygen facilitates the oxidation reactions occurring at the valence band hole by trapping the photoexcited electron at the conduction band [42] competing with mercury for the reduction reaction. Additionally, the reaction of oxygen with the cb electron generates a superoxide radical which has the potential to re-oxidize the reduced species of mercury. Therefore, an inert gas purge, such as nitrogen, is desirable to reduce the dissolved oxygen in solution

Visible Light Photocatalysis

Table 2-1 lists a few possible photocatalysts and their band gap energies. A suitable catalyst must be photoreactive at an achievable energy level, non-toxic, chemically stable and non photocorrosive [43]. Titanium dioxide (TiO_2) is the most widely used photocatalytic material; highly suitable for environmental applications [44].

Titanium dioxide exits in two crystalline structures: rutile (3.0 eV) and anatase (3.2 eV) [45]. Degussa P25 is a commercially available TiO_2 comprised of a mixture of 70% anatase and 30% rutile with an average particle size of 30 nm and BET surface

area of 40-70 m^2/g [46]. Although the band gap of TiO_2 requires photon energy at or below UVA wavelengths (< 290 nm), it has been argued that only a few photons at the required energy level are sufficient to promote photocatalysis [44]. Therefore, the small amount of UVA photons emitted by indoor lighting could perhaps be capable of generating electron-hole pairs on the surface of TiO_2 and treating trace amounts of contaminant. A series of studies investigated the photocatalytic degradation (PCD) rate of various organic compounds with respect to light intensity and were able to achieve degradation by solar radiation; however it was observed that PCD rate does increase with increasing light intensity [29] [47] [48].

Various techniques have been conducted to improve the photocatalytic potential of TiO_2 under visible light such as doping the catalyst with metal and non-metal ions [49] [50] [51] [52]. Most of the literature has focused on characterizing the modified photocatalyst and measuring light absorption/reflection [45] [52] [53] but not many studies have been published comparing side by side results of photocatalytic reduction of heavy metals under visible and ultra-violet light. If indeed only a few photons are required to excite the valence band electron, it could be argued that a visible light source would be sufficient to reduce trace levels of contaminants. Additionally, the slightly increased absorbance of light for the doped catalysts may be negligible if successful results are obtained by using plain TiO_2 under visible light. Asahi et al investigated the effects of doping titanium dioxide with nitrogen. The absorbance of light in the visible range for doped catalysts is only enhanced marginally compared to plain TiO_2 [53]. Other studies slightly improved the reflectance/absorbance of light in the

visible light range of TiO_2 by doping techniques, demonstrating insignificant difference between doped and undoped catalysts [51] [54] [55].

About 30% decomposition of rhodamine B and 2,4-dichlorophenol was achieved using pure TiO_2 under visible light [56]. Nitrogen doping of the catalyst improved results to decomposition rates between 45% and 98% depending on the nitrogen dose, however the study was conducted using high ppm concentrations of contaminants. It would be interesting to investigate the photocatalytic decomposition rate with pure TiO_2 at lower contaminant concentrations. Additionally, the contact times were as high as 5 hours, which would be unfeasible in application.

If it can be demonstrated that the photoreduction of heavy metals is possible using a visible light source, the additional costs of doping techniques and high energy UV light sources would be unnecessary for the commercial application of photocatalytic treatment of trace metals.

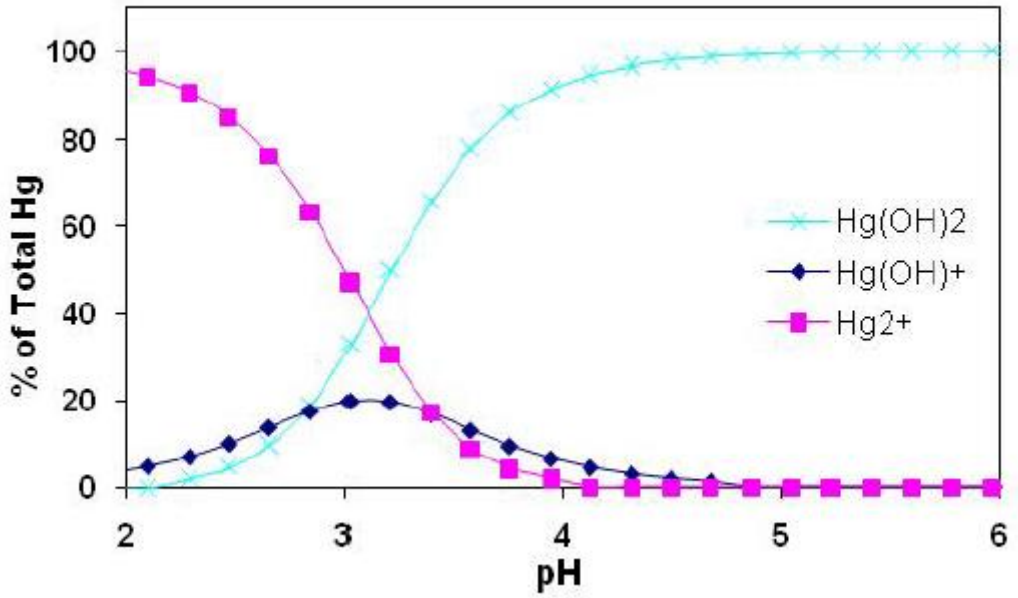

Figure 2-1. Speciation of 100 uL of Hg solution prepared from $Hg(NO_3)^2$. Adapted from: H. Byrne, Adsorption, Photocatalysis, and Photochemistry of Trace Level Aqueous Mercury, Gainesville: University of Florida, 2009.

Table 2-1. Band gap energies for different photocatalysts. Adapted from: D. Bhatkhande, V. Pangarkar and A. Beenackers, "Photocatalytic degradation for environmental applications: a review," Journal of Chem. Tech. and Biotech. , vol. 77, no. 1, pp. 102-116, 2001.

Photocatalyst	Bandgap Energy (eV)	Photocatalyst	Bandgap Energy (eV)
Si	1.1	ZnO	3.2
TiO_2 (rutile)	3	TiO_2 (anatase)	3.2
WO_3	2.7	CdS	2.4
ZnS	3.7	$SrTiO_2$	3.4
SnO_2	3.5	WSe_2	1.2
Fe_2O_3	2.2	α-Fe_2O_3	3.1

CHAPTER 3
EXPERIMENTAL

STC Synthesis

The silica-titania composite was synthesized using tetraethyl orthosilicate (TEOS) as the precursor in the sol-gel method. 50 mL of DI water (18.2 MΩ-cm), 100 mL of ethanol (Fisher, 200 proof), 4 mL of 1 M nitric acid (made from concentrated Fisher) and 70 mL of TEOS were added in a HDPE container. 8 mL of 3% wt hydrofluoric acid (diluted from 49% Fisher) was added to achieve a pore diameter of approximately 140 A. Lastly, a mass of 2.8 g of titanium dioxide (Degussa P25) was added for a TiO_2 loading of 4%. The mixture was magnetically stirred until gelation. It was then capped and allowed to age at room temperature for 4 hours and dried at 65 degrees Celsius for an additional 48 hours. The material was transferred to a Pyrex container and covered with pin-sized holes to allow moisture to escape. It was heated at a temperature of 103 degrees Celsius for 18 hours followed by 180 degrees Celsius for 6 hours. The dried material was ground using a mortar and pestle and then sieved to achieve particles between 45 to 90 μm. Table 3-1 summarizes the surface characteristics of each catalyst.

Co-mixing Studies

Hg solutions were prepared by diluting 1000 mg/L of $Hg(NO_3)_2$ (Fisher) with deionized water. Formic acid (Fisher) was added at a concentration of 1.5 ppm of carbon. Experiments were conducted in Pyrex flasks with a liquid volume of 150 mL and continuously stirred by magnetic stir bars. The STC was added at a loading of 1 g/L based on previous pseudo equilibrium batch studies [56]. Catalysts for the co-mixing experiments were added in equal amounts (0.5 mg/L of each) to achieve a total

concentration of 1 mg/L. Illuminated experiments were conducted for 5, 15 and 30 minutes exposed to visible light at a distance of 1 inch from the reactors. The bulb used was a GE Ecolux Startcoat T-8 Linear Fluorescent Light with a peak wavelength close to 550 nm (Figure 3-1) [57]. Flasks were capped with rubber stoppers equipped with a purge glass tube (5 mm diameter) and a similar vent tube (Figure 3-2). Experiments were conducted under no purge (solely exposed to air) and under nitrogen purge (Airgas, ultra high purity) at a rate of 2 L per minute controlled by a flow meter. Control experiments were conducted in the dark following the same procedure described above. The flasks were covered in aluminum foil to prevent exposure to any ambient light. Duplicate experiments were conducted for all sets and the ranges of values are expressed by error bars.

STC and TiO_2 Comparison Studies

Time dependent studies were conducted as described above. Pyrex flasks containing 150 mL of 100 ppb Hg solution were exposed to visible light under varying conditions. The STC concentration was maintained at 1 g/L and the TiO_2 concentration was determined from the loading of the material in the silica-titania composite; approximately 76 mg/L. Mixtures were exposed to one linear fluorescent visible light bulb at a distance of 1 inch from the flasks for time intervals of 5, 15 and 30 minutes. Flasks were covered with a rubber stopper equipped with 5 mm glass tubes for gas purge and ventilation. The stopper and glass tubes were present in dark experiments as well to maintain equal mixing gradients.

Lastly, the same experiments were conducted under 254 nm ultra-violet light in order to compare mercury removal in both scenarios. For these studies, a liquid volume of 100 mL was placed in a cylindrical Pyrex glass reactor and continuously stirred by

magnetic mixing (Figure 3-3). The reactors were covered with a Teflon lid equipped with two ¼ inch glass tubes; one for delivery of a gas purge and the other for ventilation. A PL-S Twin Tube Short Compact Fluorescent Lamp was inserted through the Teflon lid into the reactor. Illumination, addition of the catalyst, and the gas purge (when applicable) were initialized at the same time for all experiments.

For dose dependent studies, experiments were conducted as described above for a period of 5 minutes under the same scenarios described in Figure 3-4. The matrix of catalyst doses is presented in Table 3-2. The 0 mg dose represents the experiments exposed to visible light only, without the addition of a catalyst.

For all STC and TiO_2 comparison studies, control experiments were conducted in the dark. Additionally, comparison experiments were conducted under 254 nm ultra-violet light. Duplicate experiments were conducted for all studies and results are reported as normalized concentration C/C_0. Error bars represent the range of values obtained.

In all studies, the pH was measured but not controlled. The values ranged from 3.80 to 4.5. There was no significant change in removal between different pH values within the range.

Sample Collection and Analysis

After illumination, samples were vacuum filtered through a 45 µm cellulose membrane to separate the catalyst from the solution. Aliquots of 20 mL were taken from the filtrate and placed in 40 mL glass vials with Teflon lined caps. Nitric acid was added immediately in order to preserve the samples which were digested according to the EPA standard method 254.3 and analyzed within two weeks of collection using a Teledyne

Instruments Hydra Atomic Adsorption Mercury Analyzer manufactured by Leeman Labs. The detection limit was determined to be 1 ppb of mercury.

Table 3-1. Catalyst Surface Characterization

	BET m^2/g	Pore Size Å	Pore Vol. cc/g	Mesopore Vol. cc/g
WO_3	10.45	136.00	0.0336	0.03172
STC	174.67	182.60	0.7974	0.7826
TiO_2	45.22	194.90	0.2203	0.2046

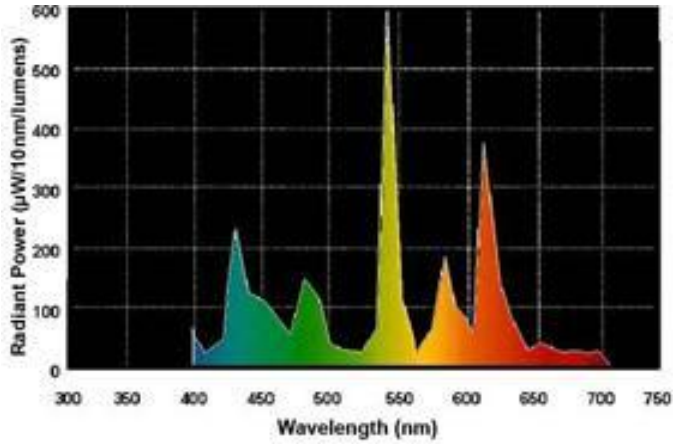

Figure 3-1. Spectral power distribution provided by the manufacturer [57]

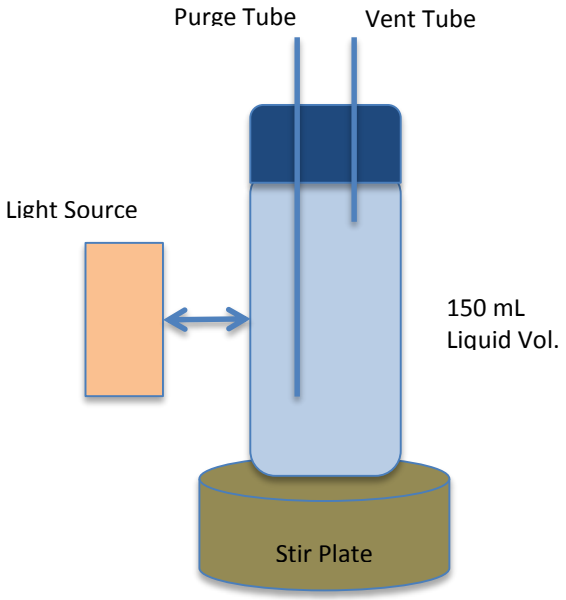

Figure 3-2. Visible light setup (profile view).

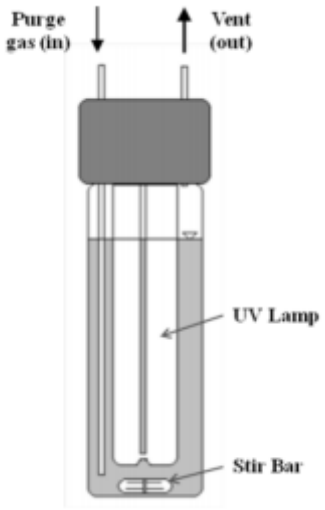

Figure 3-3. Reactor setup employed in UV 254 studies

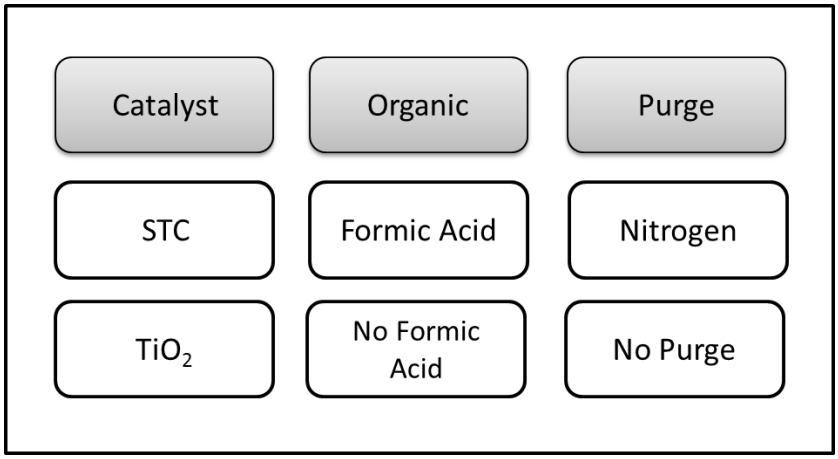

Figure 3-4. Experimental conditions for STC and TiO_2 comparison studies.

Table 3-2. Equivalent catalyst dose.

Catalyst	Dose (mg)					
TiO_2	0	2	4	6	8	10
STC	0	26	53	79	105	132

CHAPTER 4
PHOTOCHEMICAL REMOVAL OF AQUEOUS MERCURY BY CO-MIXING CATALYSTS

Control Studies

Control studies were conducted in the dark under nitrogen purge with the presence of formic acid to measure adsorption and ensure that photochemical reactions occurred when visible light was present. The removal of mercury in this scenario represents the adsorption on to the surface of the silica-titania composite. It is expected that a competition for adsorption exists between mercury and formic acid and that the removal of mercury via adsorption would increase if there was no formic acid present. However, the intention was to maintain the optimal conditions for removal under illumination to ensure the photoreduction in the presence of visible light.

The highest removal overall in the absence of light was for the co-mixed (STC+WO_3) catalyst indicating enhanced adsorption when more than one catalyst was used simultaneously (Figure 4-1). The removal of mercury ranged from 21% to 54% for STC, from 44% to 59% for WO_3 and from 45% to 69% for co-mixed STC+WO_3 for time intervals ranging from 5 minutes to 30 minutes.

Effect of Visible Light and Nitrogen Purge

The addition of visible light seems to drastically improve removal compared to the dark experiments (Figure 4-2). Removal proceeds as a first-order reaction dependent on the initial mercury concentration. This agrees with the hypothesis that higher concentrations of mercury would require more electrons produced from electron-hole pairs, therefore requiring a higher dose of UV light. As discussed in Chapter 2 (Equation 2-20), two electrons are required to reduce Hg^{2+} to Hg^0, therefore higher concentrations of Hg^{2+} would require more electrons for oxidation.

In this case, the photon energy in visible light is sufficient to decrease the concentration of mercury from 100 ppb at time zero to approximately 1 ppb at 30 minutes. The presence of a nitrogen purge slightly increased removal at the 5 minute interval but there was no significant difference at 15 or 30 minutes (Figure 4-2).

Similar results were observed for WO_3 at 15 and 30 minutes; there was a significant difference in the removal of mercury when comparing dark runs with illuminated experiments and no substantial difference in results between experiments with and without a nitrogen purge (Figure 4-3). The presence of a nitrogen purge may not be as significant in these scenarios since there is an organic compound in solution. The formic acid present acts as a hole scavenger and radical sink, preventing re-oxidation of Hg^0 to Hg^{2+} by either hydroxyl or superoxide radicals. However, this may not occur in the absence of formic acid since there would be no compound to absorb superoxide radicals formed by dissolved oxygen. The effect of nitrogen purge without an organic compound present will be discussed in subsequent sections.

The nitrogen purge, however, did affect the removal in the co-mixing experiments (Figure 4-4). At the 5 minute interval, removal was about 68% with no purge compared to 94% under nitrogen purge; showing almost 30% more removal. It was indicated in the literature that tungsten oxide has smaller band gap energy than titanium dioxide; 2.7 eV compared to 3.2 eV [43]. This would mean that more electron-hole pairs would be produced at the same energy intensity as compared to TiO_2, therefore, increasing the potential for radical formation and requiring both a nitrogen purge and organic present for effective removal. At first glance, the removal of Hg using a co-mixed catalyst seemed to improve when compared to STC or WO_3 alone. However, comparing co-

mixed data to STC in the absence of N_2 purge, under visible light shows no difference in removal (Figure 4-5).

Additionally, there was a slight improvement in adsorption of mercury for co-mixed catalysts compared to single catalysts as discussed in the control studies. Analyzing the 30 minute interval for STC and STC + WO_3 in the dark demonstrates an improvement in removal of approximately 14% (Figure 4-6). Co-mixed STC+WO_3 demonstrated high removal at all time intervals. Studies were performed using half dose of STC to verify that removal improvement was actually due to the addition of WO_3 and not the decreased dose of STC. The results show that there was no significant difference in mercury removal using 1 g/L of STC compared to 0.5 g/L. In summary, the addition of WO_3 to STC improves removal of mercury through enhanced adsorption and there is no effect on photoreduction.

Figure 4-7 summarizes the results of all experiments under nitrogen purge in the presence of formic acid. It is important to note that the silica-titania composite was successful at removing mercury under illumination with more than 80% removal at only 5 minutes and performed better than tungsten oxide. This could be explained by the same theory of why the nitrogen purge is effective for co-mixed catalysts compared to single catalysts. WO_3 displays lower band gap energy than TiO_2 creating more electron-hole pairs in visible light. The increased number of these pairs will escalate the chance of radical formation and lead to re-oxidation of mercury. Increasing the initial concentration of mercury could possibly invert removal results leading to higher removal with WO_3 compared to STC.

The next sections are devoted to understanding reduction of mercury using STC in more detail and optimizing the process by studying the effects of contaminant concentration, gas purge, presence of an organic and comparison to titanium dioxide.

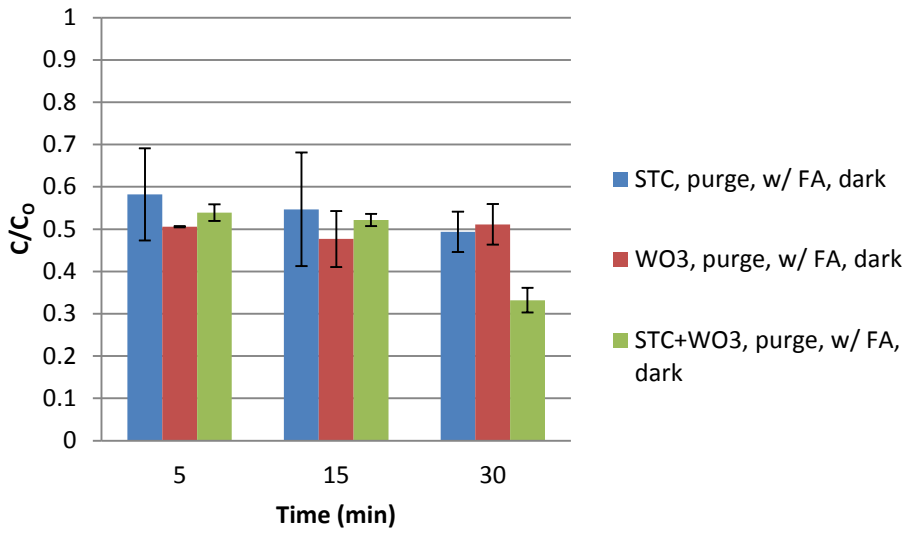

Figure 4-1. Time dependent control studies in the absence of light. Experimental conditions: 100 ppb of Hg, 1.5 ppmC of formic acid, 2 L/min nitrogen purge, 1 g/L total catalyst concentration.

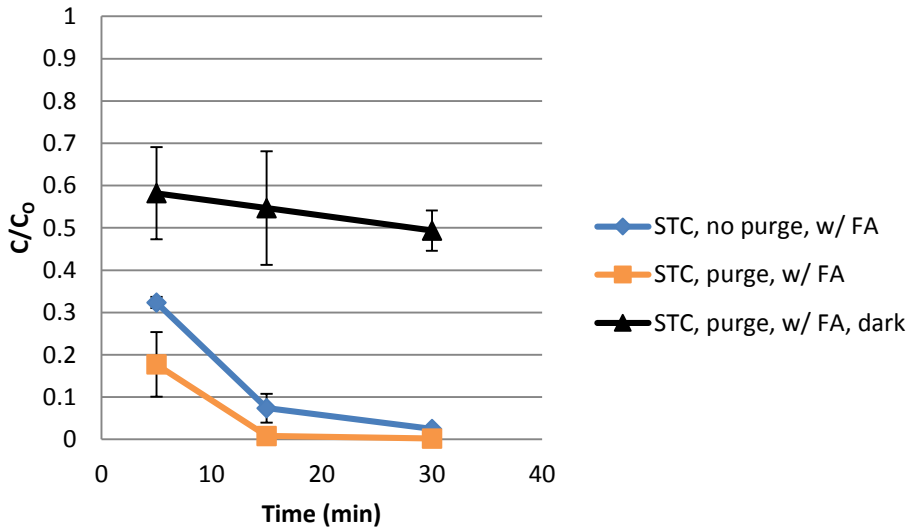

Figure 4-2. Photoreduction of mercury using STC under visible light in the presence of formic acid. Experimental conditions: 100 ppb Hg, 1.5 ppmC formic acid (FA), 2 L/min nitrogen purge, 1 g/L STC.

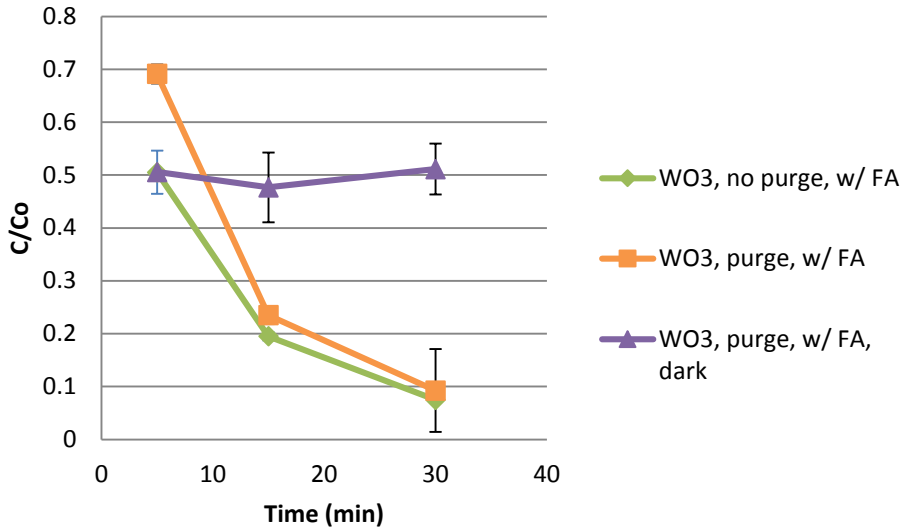

Figure 4-3. Photoreduction of mercury using WO_3 under visible light in the presence of formic acid. Experimental conditions: 100 ppb Hg, 1.5 ppmC formic acid (FA), 2 L/min nitrogen purge, 1 g/L WO_3.

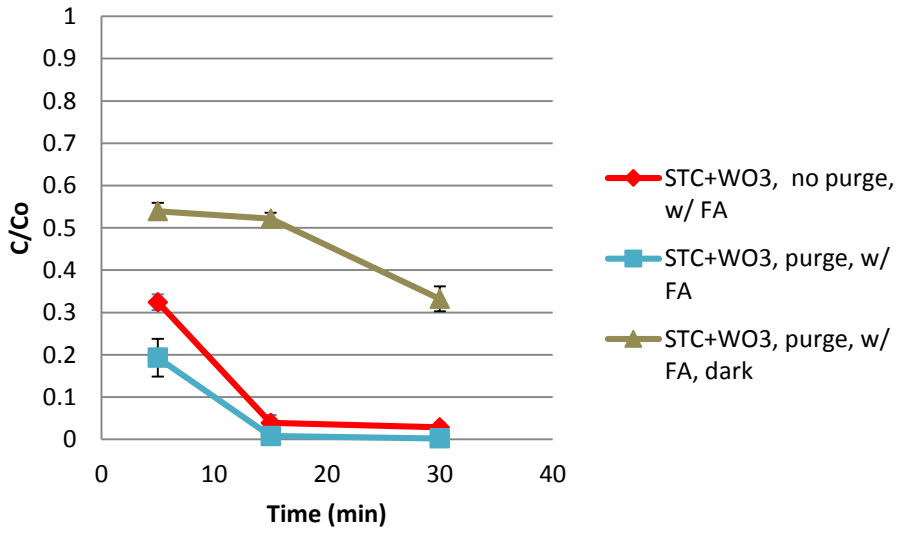

Figure 4-4. Photoreduction of Hg: effects of co-mixing silica-titania composite and tungsten oxide in the presence of formic acid. Experimental conditions: 100 ppb Hg, 1.5 ppmC formic acid (FA), 0.5 g/L of each catalyst.

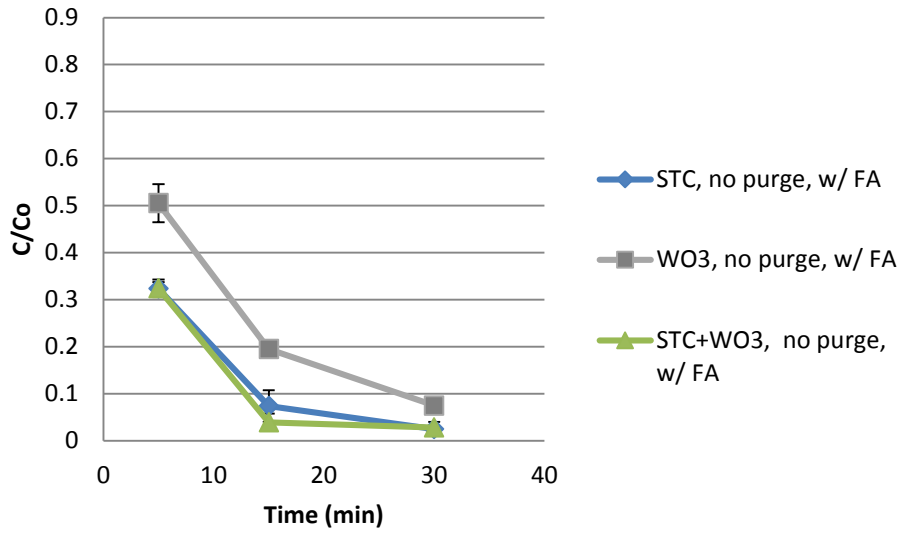

Figure 4-5. Comparison of catalysts in the absence of a nitrogen purge. Experimental conditions: 100 ppb Hg, 1.5 ppmC formic acid (FA), 1 g/L single catalyst, 0.5 g/L combined catalyst.

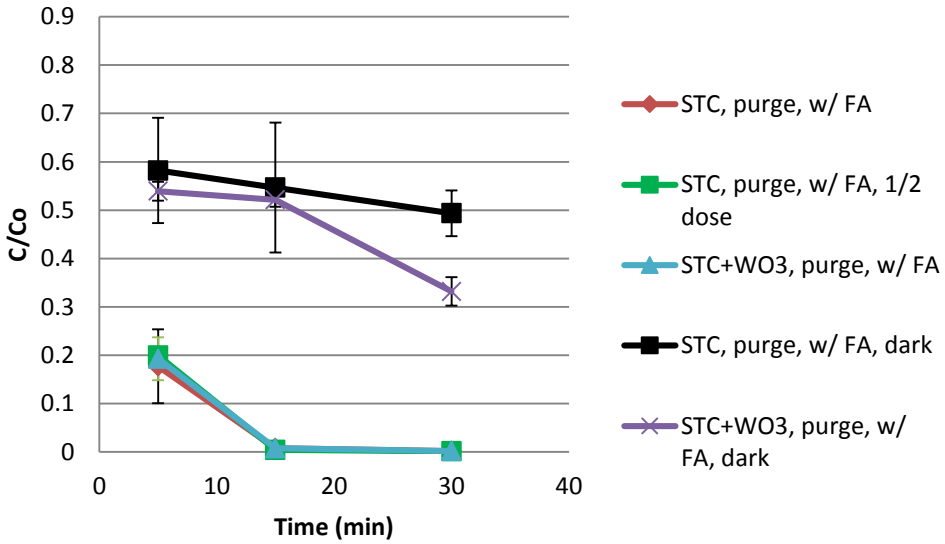

Figure 4-6. Comparison of silica-titania composite alone and co-mixed silica-titania and tungsten oxide under nitrogen purge in the presence of formic acid. Experimental conditions: 100 ppb Hg, 1.5 ppmC formic acid (FA), 2 L/min nitrogen purge.

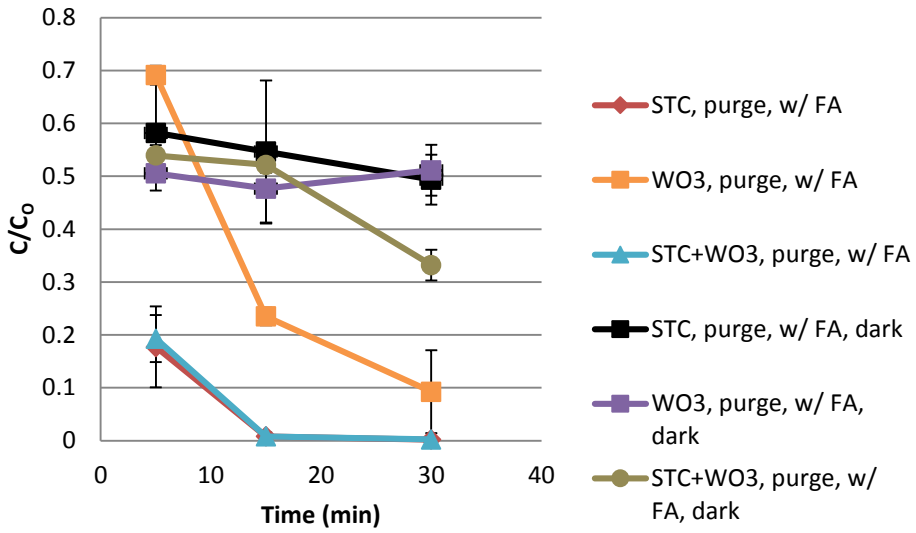

Figure 4-7. Photoreduction of mercury: comparison of all catalysts under nitrogen purge in the presence of formic acid. Experimental conditions: 100 ppb Hg, 1.5 ppmC formic acid (FA), 2 L/min nitrogen purge.

CHAPTER 5
STC AND TiO_2 TIME DEPENDENT STUDIES

Control Studies

Control studies were performed in the dark as described in the previous section to verify that reduction of mercury was due to photochemical reactions. The results are summarized in Figure 5-1. The removal of mercury by adsorption was greater using TiO_2 compared to STC for all time intervals.

Effects of Formic Acid

The effects of formic acid are described by Figure 5-2 and Figure 5-4. Removal increases by approximately 50% in the presence of formic acid compared to no formic acid under nitrogen purge within 5 minutes of illumination. However, the difference in removal is insignificant at the 15 and 30 minute intervals under the same conditions. It is hypothesized that since purge starts at time 0 (simultaneously with illumination), 5 minutes is not sufficient to completely eliminate the dissolved oxygen. The oxygen still present is competing for the conduction band electron and forming superoxide radicals that may re-oxidize the elemental species of mercury [28], [30]. On the other hand, there seems to be sufficient time at the 15 and 30 minute intervals to create a completely inert nitrogen environment making the addition of formic acid insignificant. The purge was initiated at the same time as illumination to mimic how treatment would occur is application. It would not be feasible to purge pre-treatment due to higher operational costs and longer retention times.

The importance of formic acid is emphasized in Figure 5-4 when no purge is used; removal increases significantly for all three time intervals. Formic acid reacts with the valence band hole preventing hydroxyl radical formation and acts as a sink for any

radicals present. No photocatalytic removal occurs in the absence of formic acid as seen in the comparison of dark experiments with illuminated experiments. For every divalent mercury species reduced by one electron, a radical is formed by the electron-hole pair. Since no other compound is present to react with the radical, mercury is re-oxidized to its divalent form, Hg^{2+} (Figure 5-3). Dark reactions with formic acid in the absence of a nitrogen purge were not conducted since the presence of formic acid did not significantly affect adsorption.

Effects of Nitrogen Purge

Experiments with and without formic acid were conducted to investigate the effects of a nitrogen purge under both scenarios. In the presence of formic acid, the addition of a nitrogen purge does not significantly improve results (Figure 5-5). The formic acid prevents both hydroxyl and superoxide radicals from re-oxidizing Hg^0 to its divalent form. The nitrogen purge becomes significant at longer time intervals when there is no formic acid present.

As seen in Figure 5-6, removal is the same for all scenarios at 5 minutes, when there is still dissolved oxygen present. As the purge decreases the concentration of dissolved oxygen, removal of mercury improves drastically compared to no nitrogen purge (15 and 30 minutes). Reducing the concentration of dissolved oxygen prevents the formation of superoxide radicals and since there is no formic acid present to prevent re-oxidation of Hg^0, the effect a nitrogen purge becomes more significant.

Interestingly, the silica-titania composite performed quite well in the reduction of mercury under the appropriate conditions. The studies discussed above suggest two possible mechanisms: either the silica may be responsible for lowering the band gap energy of titanium dioxide or the few photons emitted by visible light in the UVA range

are enough to cause the photocatalytic reduction of trace mercury levels. Further studies comparing STC to TiO_2 were conducted to verify a conclusion.

TiO_2 Comparison Studies

The same experiments were conducted using TiO_2 in order to compare STC's photocatalytic activity to a known, widely used catalyst. There was no significant difference in removal using STC compared to TiO_2, in the presence of formic acid and a nitrogen purge (Figure 5-7), suggesting that the silica does not alter the band gap energy of titanium dioxide. There is significance difference at the 95% confidence level for dark experiments at 30 minutes for STC and TiO_2 but this cannot be confirmed for 5 and 15 minute experiments. However, the difference in removal between the two catalysts varied greatly at 5 minutes when no formic acid was present, but this due to better adsorption of mercury onto TiO_2 nanoparticles (Figure 5-8). The data points for TiO_2 illuminated studies compared to dark studies are not statistically different at the 95% confidence level.

The presence of formic acid seems to greatly affect the removal mechanism when using titanium dioxide. If formic acid is present, photocatalysis occurs and the illuminated experiments are statistically different from the dark experiments. In the absence of formic acid, the only mechanism of mercury removal is adsorption, evident by similar dark and illuminated studies data.

Comparison of Visible Light and UV 254

Studies were conducted comparing removal using STC exposed to visible light and UV 254 nm. Removal seemed to slightly increase under UV 254 at the 5 minute interval but the difference was not statistically significant at the 95% confidence level. This suggests that a linear fluorescent bulb may be capable of generating the same

electron-hole pairs necessary to reduce mercury at a trace concentration as a compact ultra-violet bulb.

Positive results from the studies presented require further investigation to understand the photcatalytic process under visible light. More detailed experiments were conducted and discussed in the subsequent sessions focusing on the effect of dissolved oxygen, the presence of hole scavengers/radical sinks, the effect of catalyst dose contaminant initial concentration. Low doses can only be achieved by employing catalyst slurries; however, additions of dry catalysts were used for the dose dependent studies. Since the previous experiments suggest that photocatalysis may occur under visible light, it was concluded that forming a water/catalyst slurry prior to running experiments may result in the formation of radicals in the slurry.

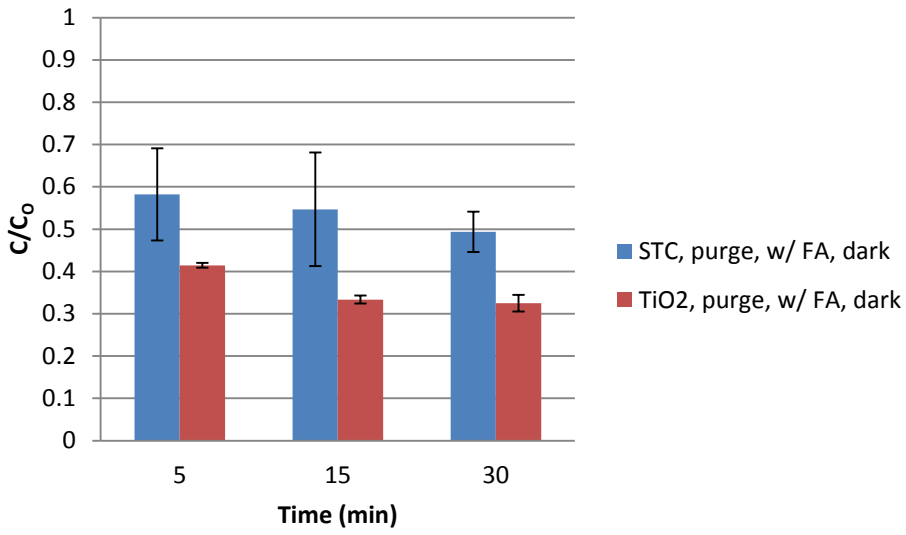

Figure 5-1. STC and TiO_2 time dependent control studies. Experimental conditions: 100 ppb of Hg, 1.5 ppmC of formic acid, 2 L/min nitrogen purge, 1 g/L STC, 76 mg/L TiO_2.

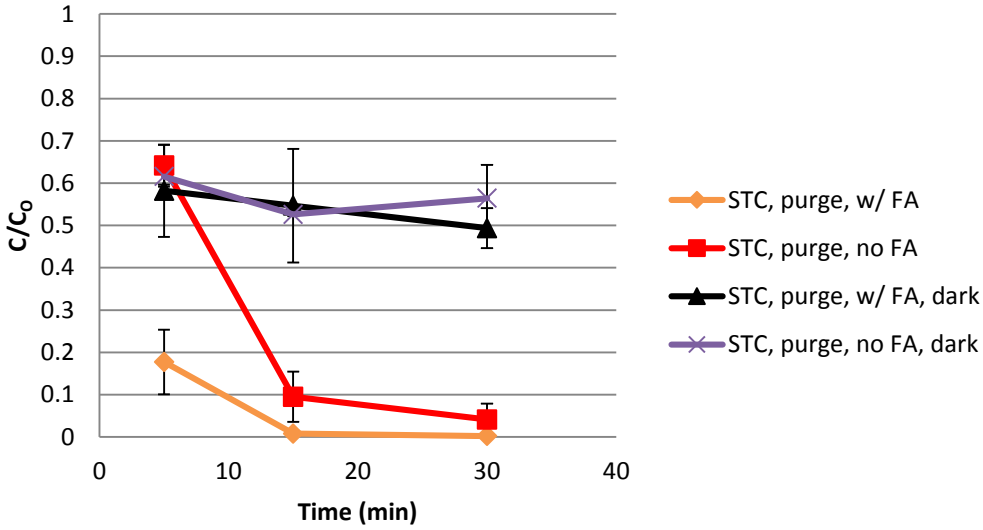

Figure 5-2. Photoreduction of mercury using STC under nitrogen purge. Experimental conditions: 100 ppb of Hg, 1.5 ppmC of formic acid (FA), 2 L/min nitrogen purge, 1 g/L STC.

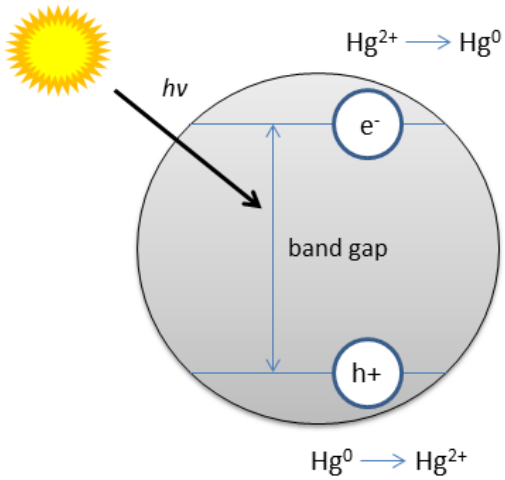

Figure 5-3. Mercury oxidation in the absence of formic acid.

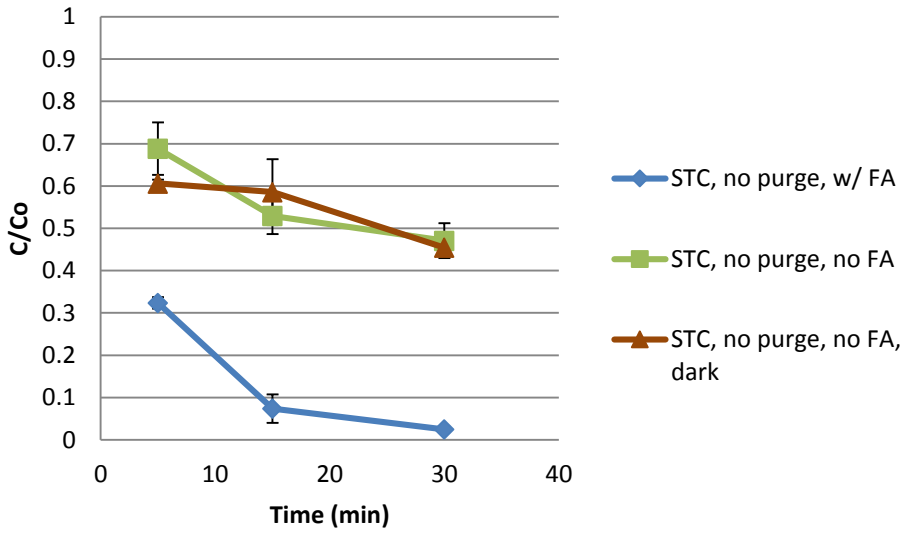

Figure 5-4. Photoreduction of mercury using STC without nitrogen purge. Experimental conditions: 100 ppb of Hg, 1.5 ppmC of formic acid (FA), 1 g/L STC, 76 mg/L TiO_2.

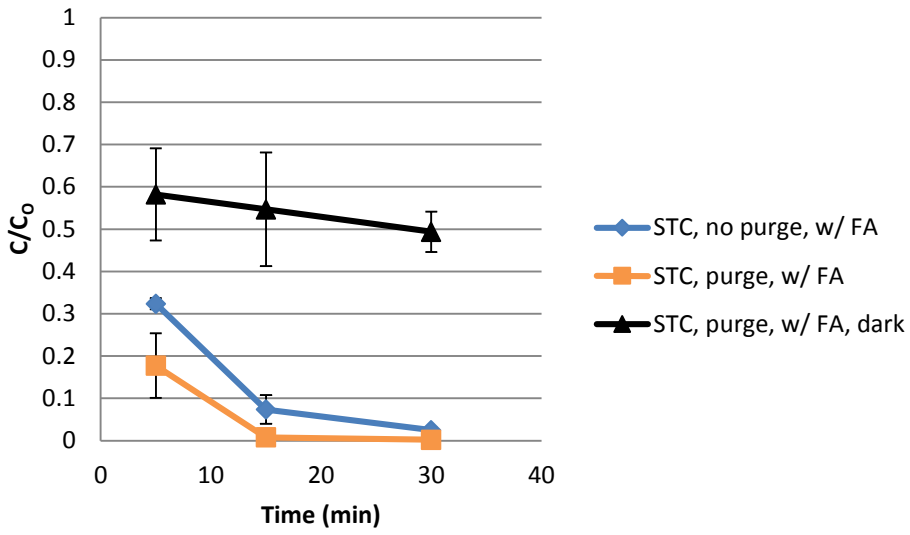

Figure 5-5. Photoreduction of mercury using STC in the presence of formic acid. Experimental conditions: 100 ppb of Hg, 1.5 ppmC of formic acid (FA), 2 L/min nitrogen purge, 1 g/L STC.

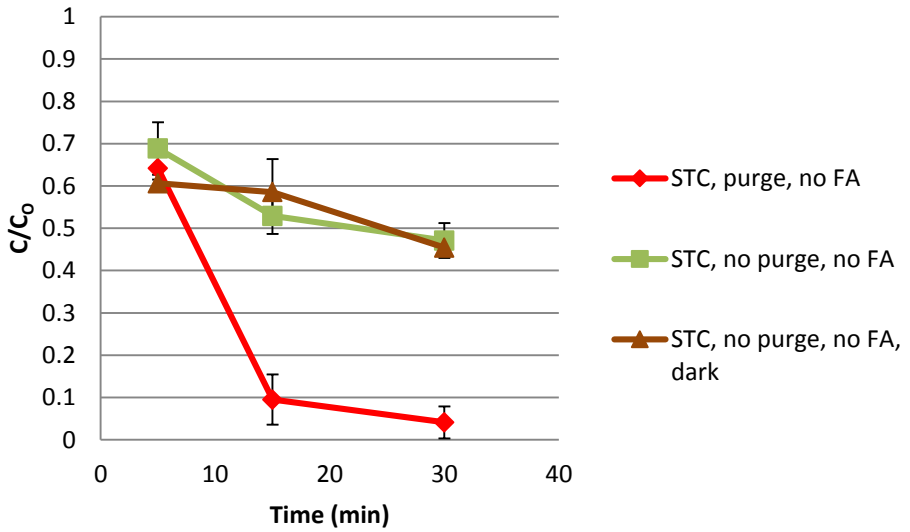

Figure 5-6. Photoreduction of mercury using STC without formic acid. Experimental conditions: 100 ppb Hg, 2 L/min nitrogen purge, 1 g/L STC.

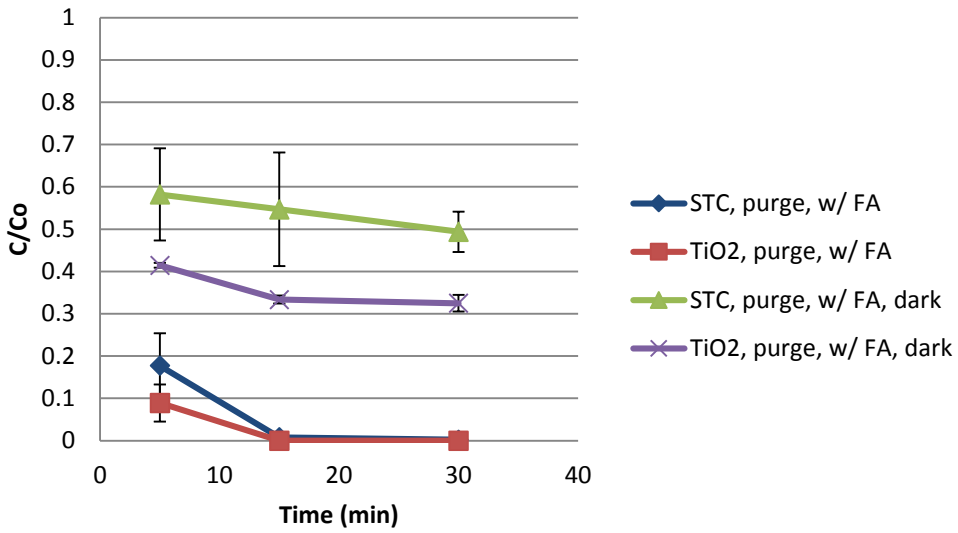

Figure 5-7. Comparison of STC and TiO2 with nitrogen purge and formic acid. Experimental conditions: 100 ppb Hg, 1.5 ppmC of formic acid (FA), 2 L/min nitrogen purge, 1 g/L STC, 76 mg/L TiO_2.

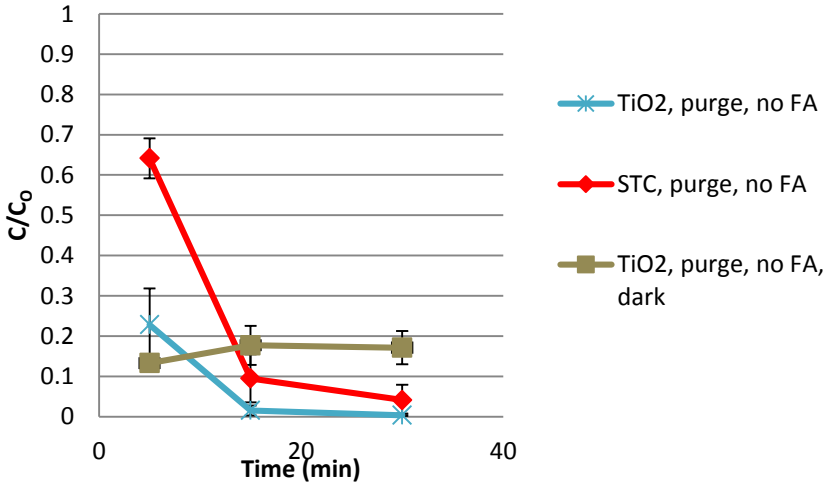

Figure 5-8. Photoreduction of mercury using TiO_2 under nitrogen purge. 100 ppb Hg, 2 L/min nitrogen purge, 1 g/L STC, 76 mg/L TiO_2.

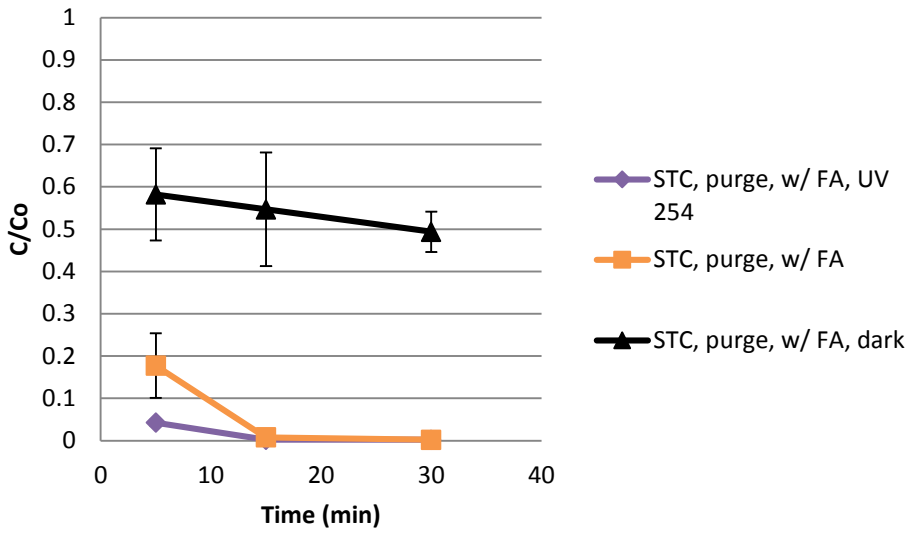

Figure 5-9. Photoreduction of mercury using STC under visible and UV 254 light. 100 ppb Hg, 1.5 ppmC formic acid (FA), 2 L/min nitrogen purge, 1 g/L STC.

CHAPTER 6
OPTIMIZATION DOSE DEPENDENT STUDIES

Control Studies and Dose Determination

Experiments were conducted in the dark with and without the addition of formic acid. It is evident from previous studies that the organic compound interferes with mercury removal (in dark runs) by competing for adsorption. The previous doses used for STC and TiO2 were 150 mg and 11.4mg respectively. This corresponded to a concentration of 1 g/L of STC and an equivalent 76 mg/L of TiO2. It was determined that the lowest, accurate mass of dry TiO2 measurable with the available balance was 2 mg. Therefore, the TiO2 doses chosen were 2, 4, 6, 8, and 10 mg. The corresponding STC doses were 26, 53, 79, 105, and132 (Table 6-1). The dose of 0 mg represents the experiments exposed to light only, without the addition of a catalyst

Effect of Formic Acid

The effects of formic acid on mercury reduction were investigated for both STC and TiO_2 with and without the presence of a nitrogen purge. The addition of formic acid did not drastically effect the removal of mercury using STC without a nitrogen purge (Figure 6-1). There seems to be a slight improvement in removal for STC doses above 50 mg. However, removal improved drastically when formic acid was added to the solution in the presence of a nitrogen purge as seen in Figure 6-2.

The nitrogen purge reduces the amount of dissolved oxygen in solution, limiting the formation of oxidizing radicals. As discussed earlier, dissolved oxygen competes with mercury for the conduction band electron. The oxygen molecule will react with the electron to form hydrogen peroxide which cleaves into hydroxyl radicals (Equations (2-6 through (2-12). Therefore, two mechanisms exits that hinder mercury reduction in the

presence of oxygen: the competition for the conduction band electron and the formation of oxidizing agents which my re-oxidize the reduced species of mercury. The addition of formic acid may reduce the amount of oxidizing agents in solution, but it will not prevent the competition for the conduction band electron as described by Equations (2-6 through (2-10 in Chapter 2.

When the amount of dissolved oxygen has been decreased by a nitrogen purge, the effects of formic acid are amplified. There is no longer a compound competing with mercury for the conduction band spot and the amount of oxidizing agents in solution is decreased. The formic acid interacts with the valence band hole to prevent the formation of radicals improving the reduction of mercury. Further research may be proposed to investigate whether increasing the concentration of formic acid may improve removal when there is dissolved oxygen present. The change in dose showed little to no effect on the removal of mercury suggesting that lower concentrations must be tested. However, achieving an accurate lower concentration may only possible by using a pre-mixed slurry which may result in the formation of additional radicals if this slurry is exposed to ambient light.

The same results were not obtained using titanium dioxide. The addition of formic acid hindered removal drastically in the absence of a nitrogen purge (Figure 6-3). As mentioned in the previous sections, formic acid competes for adsorption on to the catalyst, blocking the mercury from reaching the photo-excited electrons from the conduction band. This is evident by the drastic difference in removal between the two dark reactions. The data were statistically different at the 95% confidence level for dark and illuminated studies with no purge in the presence of formic acid. For the comparison

between illuminated and dark studies without a purge and without formic acid, all points were statistically different at the 95% confidence level except for 10 mg. Therefore, the photocatalytic reduction of mercury occurs using TiO_2 when there is no organic compound or nitrogen purge present.

Figure 6-4 shows the effects of formic acid when a purge is present. It is interesting to note that the presence of formic acid did not hinder removal in illuminated studies. The improvement of removal by the addition of formic acid under nitrogen purge was statistically significant for points 2, 4 and 10 mg but not for 6 and 8 mg (illuminated purge with no formic acid compared to illuminated purge with formic acid). Although formic acid competes with mercury for adsorption as seen in the dark studies, it does not impede the mercury compound from reaching the conduction band electron. In the absence of formic acid, removal was due to adsorption only, even in illuminated studies.

Effect of Nitrogen Purge

When formic acid is present, the addition of a nitrogen purge greatly improves the reduction of mercury using STC as seen in Figure 6-5, most likely by reducing the oxidizing radicals as discussed earlier. Formic acid alone is not capable of combating radicals formed by both the valence band hole (hydroxyl radicals) and the conduction band electron (superoxide radicals) and removal never surpasses 52% in this scenario. When the nitrogen purge is added, formation of radicals occurs only by hydroxide ions at the valence band hole.

However, when no formic acid is present, the addition of a nitrogen purge is insignificant (Figure 6-6). Enough hydroxyl radicals are formed to re-oxidize the elemental mercury species. This may support the theory that the main oxidizing agents

generated by the electron-hole pair are hydroxyl radicals formed by the interaction between water and/or hydroxide ions at the surface of the catalyst and the positive valence band hole as described by in Chapter 2 by Equations (2-4 and (2-5 [26].

Similar results were observed using TiO_2. The addition of a nitrogen purge made a drastic difference when formic acid was present (Figure 6-7) but was insignificant in the absence of formic acid (Figure 6-8). It was concluded that the generation of radicals by the dissolved oxygen affects removal negatively when there are no additional hydroxyl radicals being formed. In the absence of formic acid, radicals are being produced by the positive valence band hole at the same rate that mercury is reduced by an electron from the conduction band. Therefore, removal of mercury reaches equilibrium whether or not additional radicals are formed by the dissolved oxygen.

Figure 6-9 and Figure 6-10 summarize the results of all experiments using STC and TiO_2 respectively. By comparing results altogether, it is evident that the best mercury removal scenario using STC includes the presence of formic acid exposed to a nitrogen purge. For TiO_2, the difference is not as drastic, but the best removal environment also includes the combination of formic acid with a nitrogen purge. For TiO_2, studies with no formic acid and no nitrogen purge performed just as well as having both components present, but it was concluded that removal was due to adsorption only.

Table 6-1. Catalyst doses for dose dependent studies.

Catalyst	Dose (mg)					
TiO2	0	2	4	6	8	10
STC	0	26	53	79	105	132

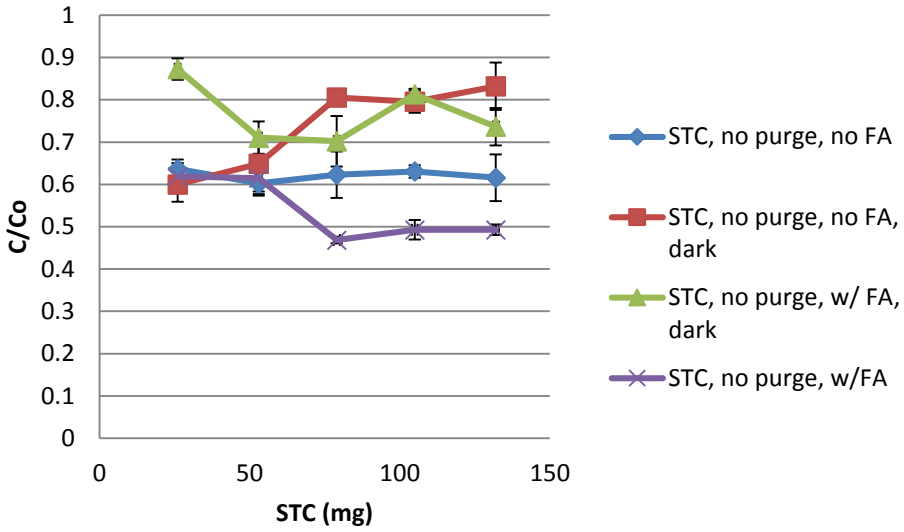

.

Figure 6-1. Effects of formic acid on photoreduction of mercury using STC without a purge. Experimental conditions: 100 ppb of Hg, 1.5 ppmC formic acid (FA), 5 min.

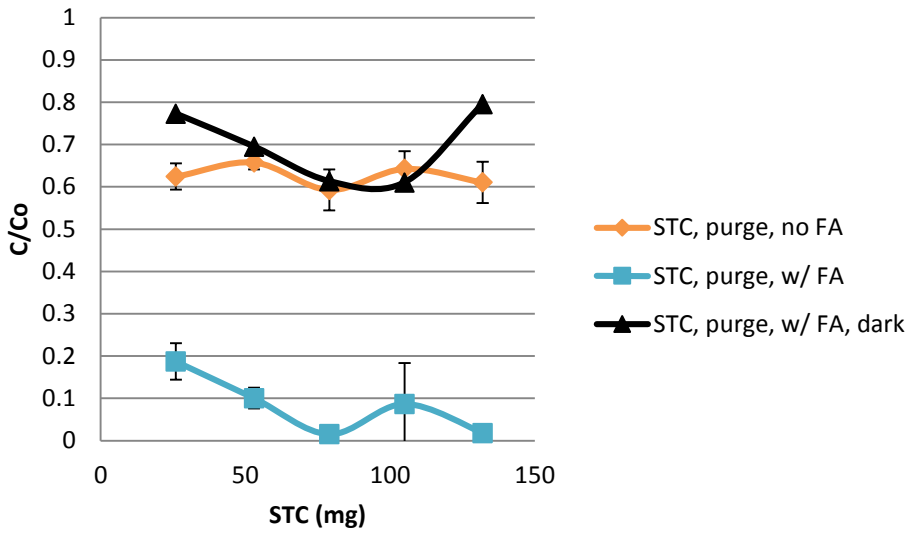

Figure 6-2. Effects of formic acid on photoreduction of mercury using STC under nitrogen purge. Experimental conditions: 100 ppb Hg, 1.5 ppmC formic acid (FA), 2L/min purge, 5 min.

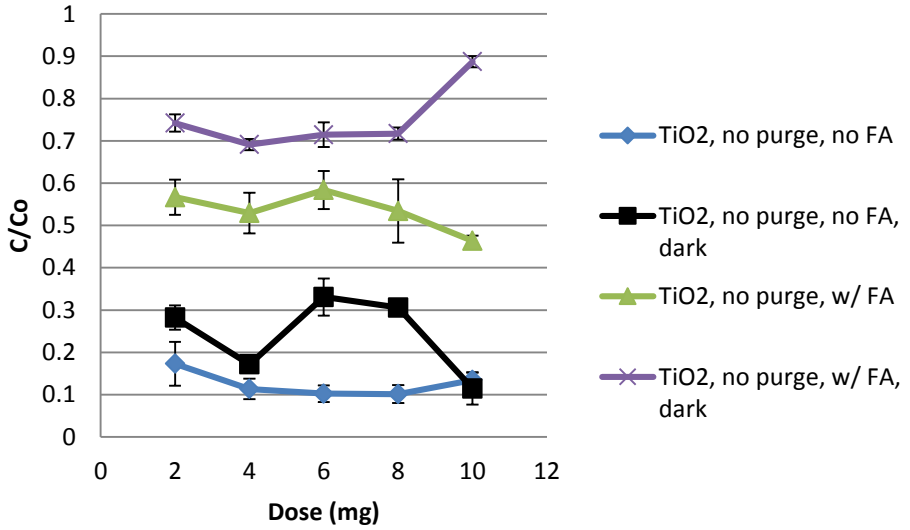

Figure 6-3. Effects of formic acid on photoreduction of mercury using TiO_2 without nitrogen purge. Experimental conditions: 100 ppb Hg, 1.5 ppmC formic acid (FA), 5 min.

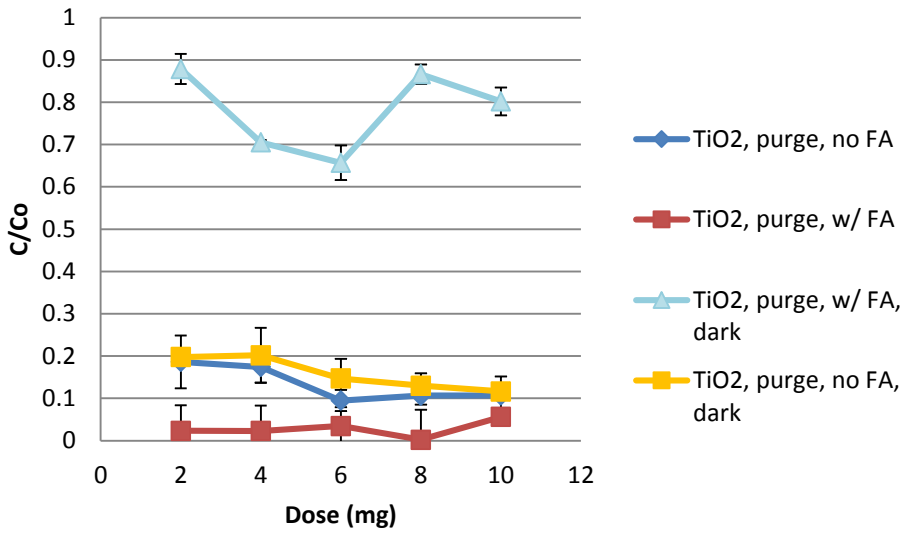

Figure 6-4. Effects of formic acid on photoreduction of mercury using TiO_2 under nitrogen purge. Experimental conditions: 100 ppb Hg, 1.5 ppmC formic acid (FA), 2 L/min nitrogen purge, 5 min.

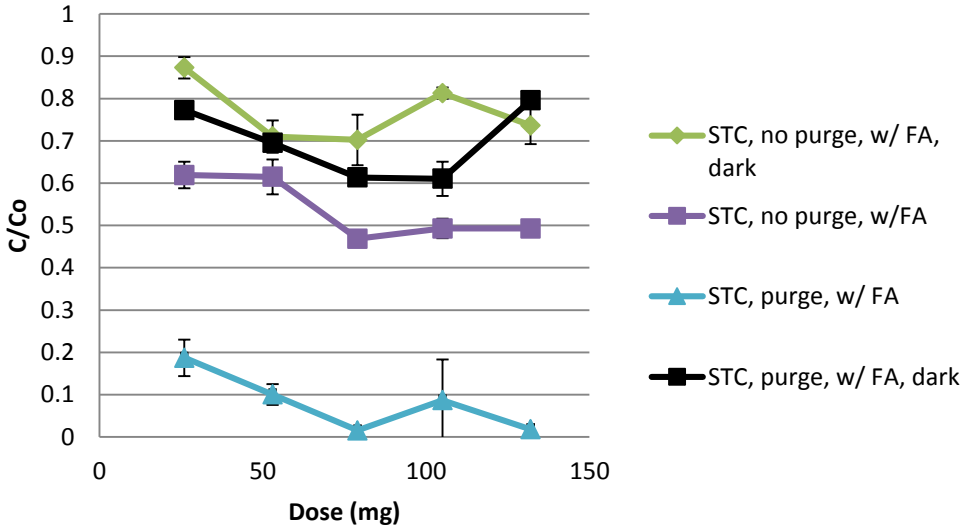

Figure 6-5. Effects of nitrogen purge on photoreduction of mercury using STC with formic acid. Experimental conditions: 100 ppb Hg, 1.5 ppmC of formic acid (FA), 2 L/min purge, 5 min.

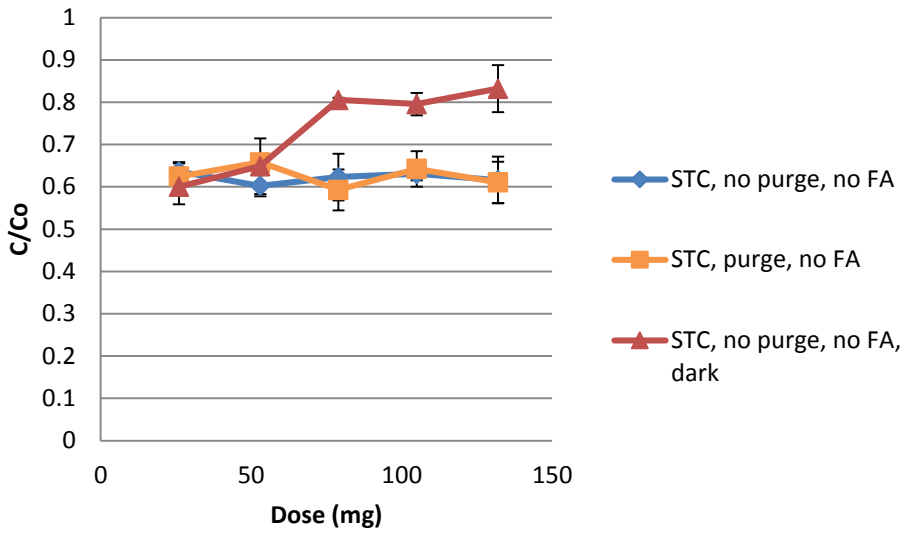

Figure 6-6. Effects of nitrogen purge on photoreduction of mercury using STC with no formic acid. Experimental conditions: 100 ppb Hg, 2 L/min nitrogen purge, 5 min.

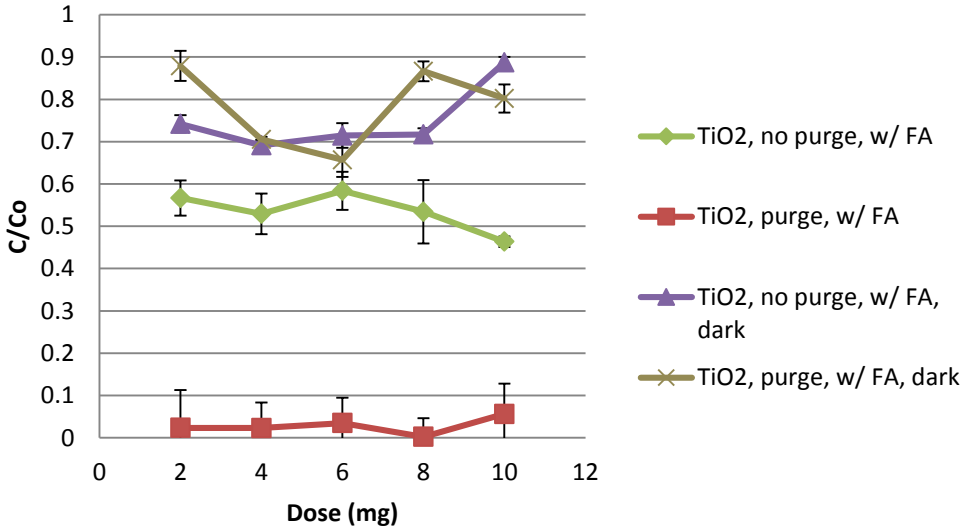

Figure 6-7. Effects of nitrogen purge of photoreduction of mercury using TiO_2 with formic acid. Experimental conditions: 100 ppb of Hg, 1.5 ppmC formic acid (FA), 2 L/min nitrogen purge, 5 min.

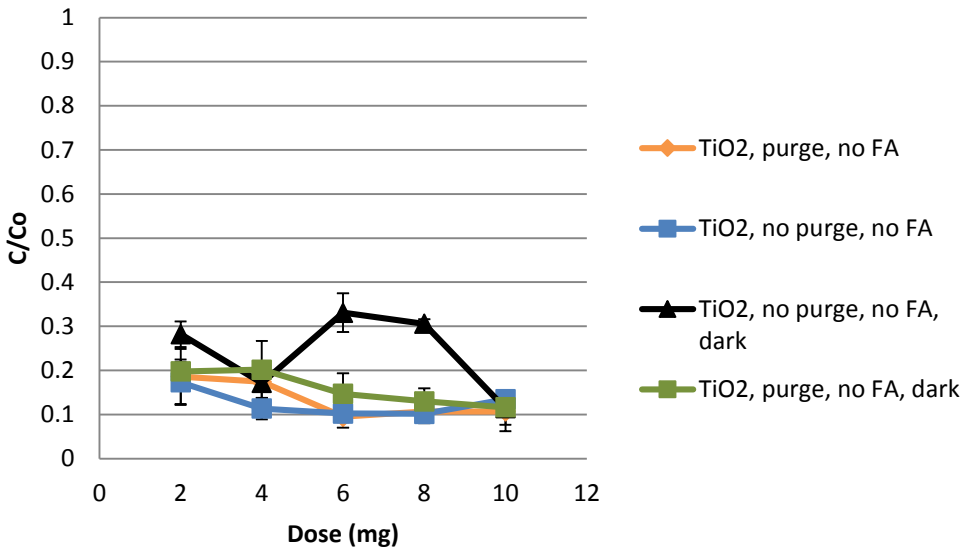

Figure 6-8. Effects of nitrogen purge on photoreduction of mercury using TiO_2 without formic acid. Experimental conditions: 100 ppb of Hg, 2 L/min nitrogen purge, 5 min.

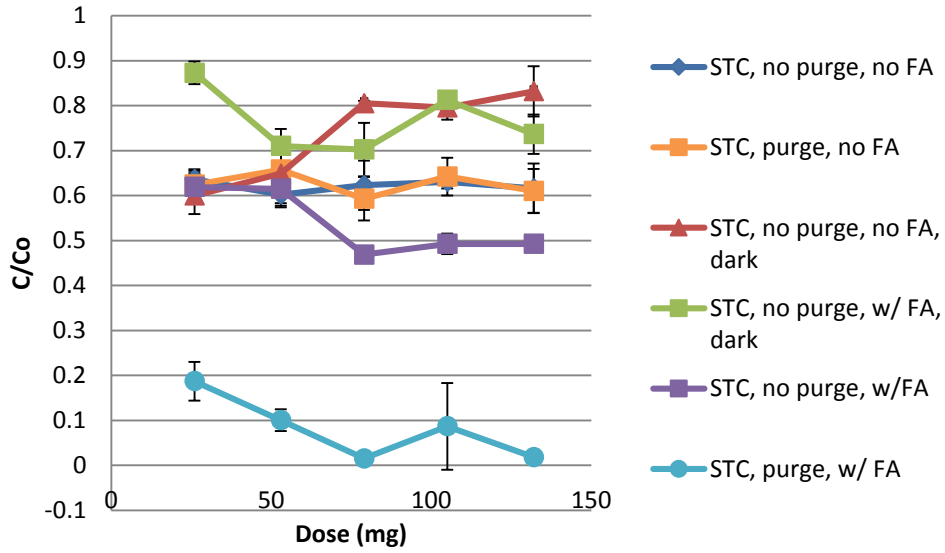

Figure 6-9. Photoreduction of mercury using STC: comparison on all scenarios.

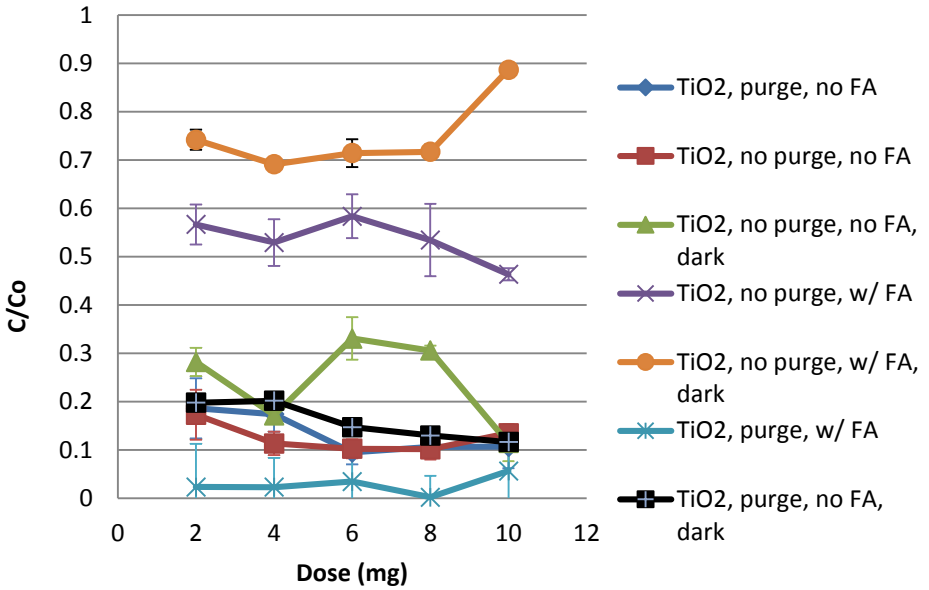

Figure 6-10. Photoreduction of mercury using TiO_2: comparison of all scenarios.

CHAPTER 7
MERCURY CONCENTRATION DEPENDENT STUDIES

Control Studies

Studies were conducted in the dark with mercury initial concentrations of 100, 500 and 1000 parts per billion. The catalyst concentration was 1 g/L for STC and the equivalent 76 mg/L for TiO_2. Experiments were conducted in the presence of formic acid and nitrogen purge for 5 minutes. STC and TiO2 performed similarly with an initial concentration of 500 ppb of Hg; removing less than 20%. STC outperformed TiO_2 at the higher concentration of 1000 ppb (Figure 7-1).

Comparison of Visible Light vs. UV 254

Experiments were conducted for all three concentrations using STC (Figure 7-2) and TiO_2 (Figure 7-3) exposed to visible light and UV 254. As hypothesized, removal of mercury increased as initial concentration decreased when using visible light. At an initial concentration of 100 ppb, there was no statistical difference in removal using visible light compared to UV 254. Utilizing visible light source is just as effective in reducing mercury at low concentrations compared to ultra-violet light. A lower concentration of 50 ppb was investigated using STC (Figure 7-4). There was no statistical difference in removal between visible light and UV 254 at this concentration reinforcing the conclusion the visible light is capable of photoreducing low concentrations of mercury.

Two electrons are required to reduce Hg^{2+} to Hg^0. The electrons are provided by the surface of the photocatalyst after excitation by light. Since the excitation of electrons is directly proportional to the number of photons in the required energy level (370-380 nm), the reduction of mercury will also be directly proportional to the amount of photons.

If higher concentrations of mercury exist (more Hg^{2+}), then more electrons will be required for reduction. Visible light emits only a limited number of UVA photons, therefore, sufficient electrons would not be produced to reduce higher mercury concentrations. Figure 7-5 portrays a representation of the photocatalytic reduction of higher concentrations of aqueous mercury (above 100 ppb).

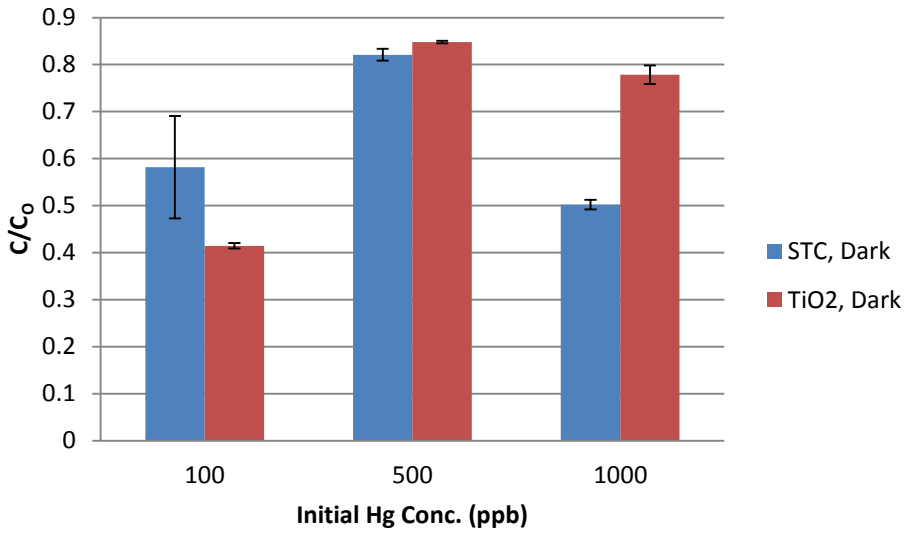

Figure 7-1. Mercury concentration dependent control studies. Experimental conditions: 1 g/L STC, 76 µg/L TiO_2, 1.5 ppm formic acid, 2 L/min nitrogen purge, 5 min.

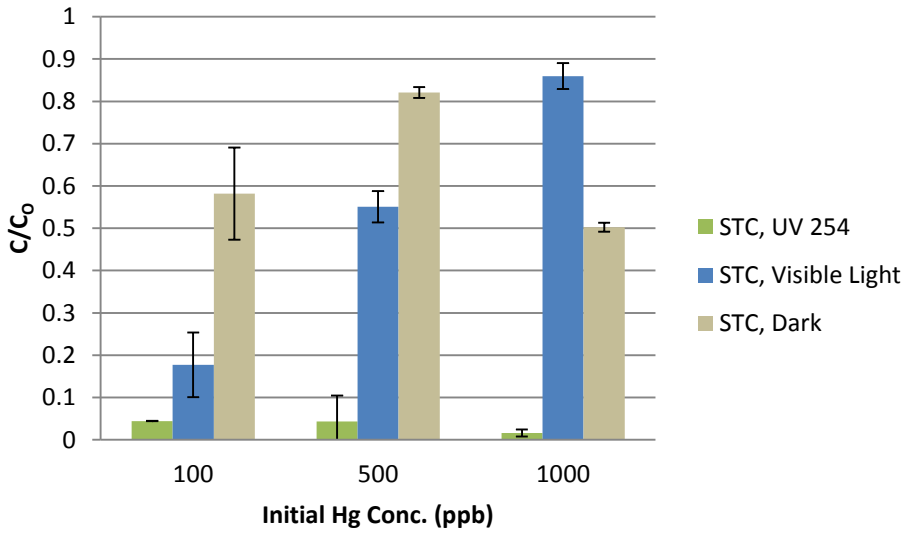

Figure 7-2. Comparison of UV 254 vs. visible light using STC. Experimental conditions: 1g/L STC, 1.5 ppmC formic acid, 2 L/min nitrogen purge, 5 min.

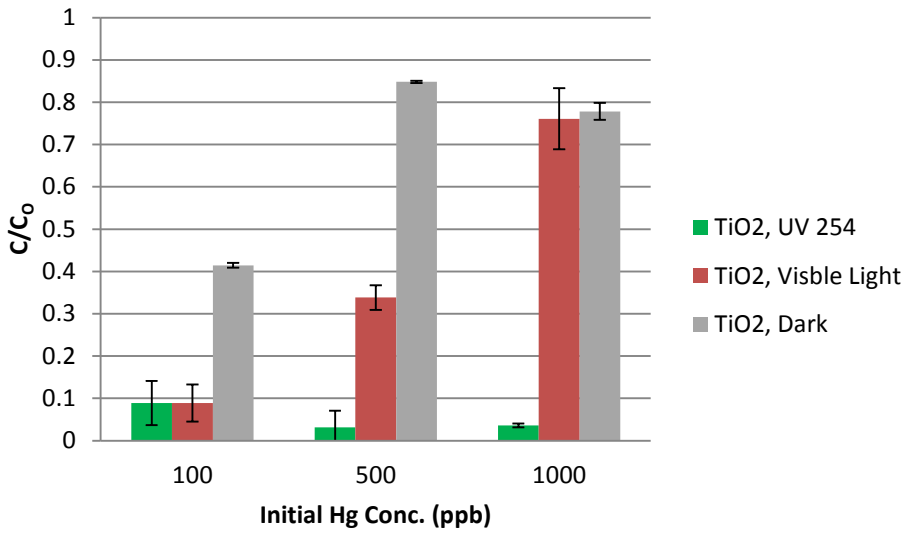

Figure 7-3. Comparison of UV 254 vs. visible light using TiO_2. Experimental conditions: 76 µg/L TiO_2, 1.5 ppmC formic acid, 2 L/min nitrogen purge, 5 min.

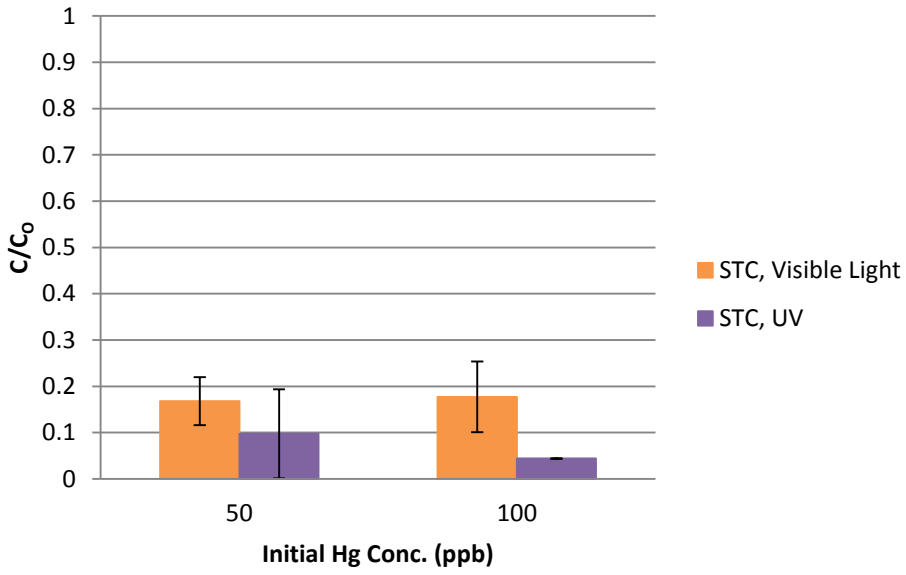

Figure 7-4. Comparison of visible light vs. UV 254 using STC at lower Hg concentrations. Experimental conditions: 1g/L STC, 1.5 ppm formic acid, 2 L/min nitrogen purge, 5 min.

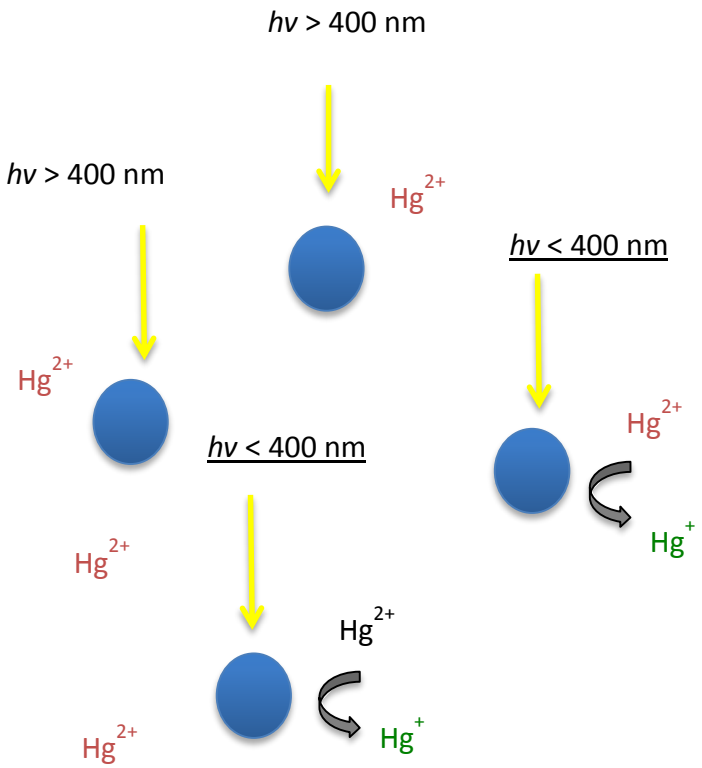

Figure 7-5. Representation of photocatalytic reduction of high concentrations of aqueous mercury.

CHAPTER 8
CONCLUSIONS

The purpose of this study was to enhance visible light photocatalysis by modifying the removal process rather than modifying the catalyst, The co-mixing of different catalysts does not affect the photocatalytic removal of mercury. The slightly increased removal evident in the co-mixed STC+WO_3 studies was due to enhanced adsorption. However, the silica-titania composite performed quite well as a single catalyst under visible light and the positive results lead to further investigation, including comparison with regular titanium dioxide.

STC and TiO_2 performed similarly in illuminated experiments with visible light suggesting that silica does not lower the band gap energy of TiO_2. Studies were conducted in different scenarios in order to understand the effect of dissolved oxygen, the presence of an organic compound and catalyst dose. It was concluded that the addition of formic acid greatly improved removal by acting as a radical sink, preventing the re-oxidation of Hg^0 to Hg^{2+}. Dissolved oxygen only affected removal negatively if formic acid was present. In the absence of an organic compound, re-oxidation of mercury occurred whether or not there was dissolved oxygen.

Lastly, it was determined that visible light is capable of emitting enough photons to reduce trace levels of mercury. Results showed similar removal using visible light compared to UV 254 at low initial concentrations of mercury (100 ppb), but poor removal at high initial concentrations of 1000 ppb. It is suggested that visible light emits few photons at a range slightly below 400 nm which may be capable of producing some electron-hole pairs. Future work may be conducted to create a model of light intensity needed based on contaminant concentrations.

Visible light photocatalysis may be employed as a polishing step to further reduce contaminant concentrations. Cheaper, more widely used process such as precipitation and carbon adsorption can reduce the bulk of contaminants found in various waste streams but these methods may not be feasible to reduce levels below the parts per billion range. Visible light photocatalysis provides a safe method of reducing multiple contaminants through both oxidation and reduction reactions.

LIST OF REFERENCES

[1] M. Fujiki and S. Tajima, "The pollution of Minamata Bay by mercury," Water Sci. Tech., vol. 25, no. 11, pp. 133-140, 1992.

[2] K. Eto, "Minamata Disease," Neuropathology, vol. 20, no. 1, pp. 14-19, 2000.

[3] U.S. Environmental Protection Agency, "Basic Information about Mercury in Drinking Water," May 2012. [Online]. Available: http://water.epa.gov/drink/contaminants/basicinformation/mercury.cfm. [Accessed January 2014].

[4] United Nations Environmental Programme, "Minamata Convention on Mercury," October 2013. [Online]. Available: http://www.mercuryconvention.org/Portals/11/documents/publications/MinamataConventiontextEn.pdf. [Accessed January 2014].

[5] M. Amyot, G. Mierle, D. Lean and D. McQueen, "Sunlight-induced formation of dissolved gaseous mercury in lake waters," Environ. Sci. Tech., vol. 28, pp. 2366-2371, 1994.

[6] UNEP, "Global mercury assesment report," United Nations Environmental Programme, New York, 2002.

[7] E. G. Pacyna, J. M. Pacyna, K. Sundseth, J. Munthe, K. Kindbom, S. Wilson, F. Steenhuisen and P. Maxson, "Global emission of mercury to the atmosphere from antropogenic sources in 2005 and projections to 2020," Atmospheric Environment, vol. 44, no. 20, pp. 2487-2499, 2010.

[8] S. Serre and G. Silcox, "Adsorption of elemental mercury on the residual carbon in coal fly ash," Ind. Chem. Eng. Res., vol. 39, no. 6, pp. 1723-1730, 2000.

[9] M. Galperin, M. Sofiev and E. Mantseva, "A model of the chemical transformation of mercury and its long-range atmospheric transport," in Global and regional mercury cycles: sources, fluxes and mass balances, Dordretch, The Netherlands, Kluwer Academic Publishers, 1996.

[10] U.S. Environmental Protection Agency, "Clean Air Mercury Rule," March 2011. [Online]. Available: http://www.epa.gov/camr/. [Accessed January 2014].

[11] U.S. Environmental Protection Agency, "Mercury and Air Toxics Standards Basic Information," April 2012. [Online]. Available: http://www.epa.gov/mats/basic.html. [Accessed January 2014].

[12] U.S. Environmental Protection Agency, "Impaired Water and Total Maximum Daily Loads," December 2013. [Online]. Available: http://water.epa.gov/lawsregs/lawsguidance/cwa/tmdl/. [Accessed January 2014].

[13] P. Tchounwou, W. Ayensu, N. Ninashvili and D. Sutton, "Environmental Exposure to Mercury and its Toxicopathologic Implications for Purblic Health," Env. Toxicology, vol. 18, no. 3, 2003.

[14] T. Clarkson, "Metal toxicity in the central nervous system," Env. Health Perspectives, vol. 75, pp. 59-64, 1987.

[15] S. Witt, "OSHA safety hazard information bulletin on dimethylmercury," [Online]. Available: http://www.osha.gov/dts/hib/hib_data/hib19980309.html.

[16] World Health Organization, "Methylmercury. International Program on Chemical Safety," Geneva , 1990.

[17] Harada, "Congenital Minamata disease: intrauterine methylmercury poisoning," Teratology, vol. 18, no. 2, pp. 285-288, 1978.

[18] Y. Harada, "Congenital (or fetal) Minamata disease.," Kumamato University, Kumamato, Japan, 1968.

[19] C.-J. Lin and S. Pehkonen, "The chemistry of atmospheric mercury: a review," Atmospheric Environment, vol. 33, pp. 2067-2079, 1999.

[20] O. Lindqvist and H. Rodhe, "Atmospheric Mercury - a reveiw," Tellus, vol. 37, no. B, pp. 136-159, 1985.

[21] F. Morel, A. Kraepiel and M. Amyot, "The Chemical Cycle and Bioaccumulation of Mercury," Annual Review of Ecology and Systematics, vol. 29, pp. 543-566, 1998.

[22] H. Hahne and W. Kronntje, "Significance of pH and Chloride Concentration on Behavior of Heavy Metal Pollutants: Mercury (II), Cadmium (II), Zinc (II), and Lead (II)," Journal of Environmental Quality, vol. 2, no. 4, pp. 444-450, 1973.

[23] H. Byrne, Adsorption, Photocatalysis, and Photochemistry of Trace Level Aqueous Mercury, Gainesville: University of Florida, 2009.

[24] K. Kabra, R. Chaudhary and R. Sawhney, "Treatment of hazardous inorganic and organic compounds through aqueous phase photocatalysis," Ind. Eng. Chem. Res., vol. 43, pp. 7683-7696, 2004.

[25] O. Legrini , E. Oliveros and A. M. Braun, "Photochemical Processes for Water Treatment," Chem. Rev., vol. 93, pp. 671-698, 1993.

[26] R. W. J. Matthews, "Hydroxylation reactions induced by near-ultraviolet photolysis of aqueous titanium dioxide suspensions," Chem. Soc. Faraday Trans., vol. 80, p. 457, 1984.

[27] R. Bickley, T. Gonzalez-Carreno, J. Lees, L. Palmisiano and R. Tilley, "A structural inverstigation of titanium dioxide photocatalyts," Journal of Solid State Chem., vol. 92, pp. 178-190, 1990.

[28] M. Litter, "Heterogeneous photocatalysis, transition metal ions in photocatalytic systems," Applied Catalysis B: Environmental , vol. 23, pp. 89-114, 1999.

[29] K. Okamoto, Y. Yamamoto, H. Tanaka and A. Itaya, "Kinetics of heterogeneous photocatalytic decomposition of phenol over anatase TiO2 powder," Bull Chem Soc., vol. 58, pp. 2023-2028, 1985.

[30] R. Cundall, R. Rudham and M. Salim, "Photocatalytic oxidation of propan-2-ol in the liquid phase by rutile," J. Chem. Soc., Faraday Trans. , vol. 72, pp. 1642-1651, 1976.

[31] P. Harvey, R. Rudham and S. Ward, "Photocatalytic oxidation of liquid propan-2-ol by titanium dioxide," J. Chem. Soc., Faraday Trans. 1, vol. 79, pp. 1381-1390, 1983.

[32] L. B. Khalil, W. E. Mourad and M. W. Rophael, "Photocatalytic reduction of environmental pollutant Cr(VI) over some semiconductors under UV/visible light illumination," Applied Catalysis B: Environmental , vol. 17, no. 3, pp. 267-273, 1998.

[33] K. Rajeshwar, C. R. Chenthamarakshan and Y. M. Wenjian Sun, "Cathodic photoprocesses on titania films and in aqueous suspensions," Journal of Electoanalytical Chemistry, Vols. 538-539, pp. 173-182, 2002.

[34] X. Wang, S. Pehkonen and A. Ray, "Photocatalytic reduction of Hg(II) on commercial TiO2 catalysts," Electrochemica Acta, vol. 49, no. 9-10, pp. 1435-1444, 2004.

[35] M. Ward, J. White and A. Bard, "Electrochemical investigation of energetics of particulate titanium dioxide photcatalysts. The methyl-viologen acetate system," J. Am. Chem. Soc., vol. 105, pp. 27-31, 1983.

[36] Y. Xu and M. Shoonen, "The absolute energy positions of conduction and valence bands of selected semiconducting minerals," American Mineralogist , vol. 85, no. 3-4, pp. 543-556, 2000.

[37] S. Sanuki, K. Shako, S. Nagaoka and H. Majima, "Photocatalytic reduction of Se ions using suspended anatase powders," Mat. Trans., JIM, vol. 41, no. 7, pp. 799-805, 2000.

[38] N. Serpone, Y. K. Ah-You, T. P. Tran and R. Harris, "AM 1 simulated sunlight photoreduction and elimination of Hg (II) and CH3Hg(II) chloride salts from aqueous suspensions of titanium dioxide," Solar Energy, vol. 39, no. 6, pp. 491-498, 1987.

[39] S. Botta, D. Rodriguez, A. Leyva and M. Litter, "Feature of the transformation og Hg(II) by heterogeneous photocatalysis over TiO2," Catalysis Today, vol. 76, no. 2-4, pp. 247-258, 2002.

[40] T. Tan, D. Beydoun and R. Amal, "Effects of organic hole scavengers on the photocatalytic reduction of selenium ions," Journal of Photochem. and Photobio. A: Chemistry, vol. 159, pp. 273-280, 2003.

[41] S. Rengaraj and X. Z. Li, "Enhanced photocatalytic reduction reaction over Bi3+-TiO2 nantoparticles in the presence of formic acid as a hole scavenger," Chemosphere, vol. 66, no. 5, pp. 930-938, 2007.

[42] M. A. Fox and M. Dulay, "Heterogenous photocatalysis," Chem. Rev., vol. 93, pp. 341-357, 1993.

[43] D. Bhatkhande, V. Pangarkar and A. Beenackers, "Photocatalytic degradation for environmental applications: a review," Journal of Chem. Tech. and Biotech. , vol. 77, no. 1, pp. 102-116, 2001.

[44] A. Fujishima, T. Rao and D. Tryk, "Titanium dioxide photocatalysis," Journal of Photochem. and Photobio. C: Photochem. Reviews, vol. 1, no. 1, pp. 1-21, 2000.

[45] J. B. Varley, A. Janotti and C. G. Van de Walle, "Mechanism of visible-light photocatalysis in nitrogen-doped TiO2," Advanced Materials, vol. 23, no. 20, pp. 2343-2347, 2011.

[46] D. Chen and A. Ray, "Removal of toxic metal ions from wastewater by semiconductor photocatalysis," Chem. Eng. Sci., vol. 56, no. 4, pp. 1561-1570, 2001.

[47] J. Critteden, J. Liu, D. Hand and D. Perram, "Photocatalytic oxidation of chlorinated hydrocarbons in water," Water Res. , vol. 31, pp. 429-438, 1997.

[48] D. Ollis, E. Pellizzetti and N. Serpone, "Destruction of water contaminants," Env. Sci. Technol., vol. 25, pp. 1523-1528, 1991.

[49] M. Seery, R. George, P. Floris and S. Pillai, "Silver doped titanium dioxide nanomaterials for enhanced visible light photocatalysis," Journal of Photochem. and Photobio. A: Chemistry, vol. 189, no. 2-3, pp. 258-263, 2007.

[50] D. Chatterjee and S. Dasgupta, "Visible light induced photocatalytic degradation of organic pollutants," Journal of Photochem. and Photobio. C: Photchem. Reviews, vol. 6, pp. 186-205, 2005.

[51] T. Umebayashi, T. Yamaki, H. Itoh and K. Asai, "Bad gap narrowing of titanium dioxide by sulfur doping," Applied Physics Letters, vol. 81, no. 3, p. 454, 2002.

[52] M. Mrowetz, W. Balcerski, A. J. Colussi and M. Hoffmann, "Oxidative power of nitrogen-doped TiO2 photocatalysts under visible light illumination," J. Phys. Chem. B , vol. 108, no. 45, pp. 17269-17273, 2004.

[53] R. Asahi, T. Morikawa, T. Ohwaki, K. Aoki and Y. Taga, "Visible-light photocatalysis in nitrogen-doped titanium oxides," Science, vol. 293, p. 269, 2001.

[54] C.-y. Wany, C. Bottcher, D. Bahnemann and J. Dohrmann, "A comparative study of nanometer sized Fe(III)-doped TiO2 photocatalysis: synthesis, characterization and activity," J. Mater. Chem., vol. 13, pp. 2322-2329, 2003.

[55] M. Liu, X. Qiu, M. Miyauchi and K. Hashimoto, "Cu(II) oxide amorphous nanoclusters grafted Ti3+ self-doped TiO2: an efficient visible light photocatalyst," Chem. of Mat., vol. 23, pp. 5282-5286, 2011.

[56] H. Byrne and D. Mazyck, "Removal of trace levels of aqueous mercury by adsorption and photocatalysis on silica-titania composites," Journal of Hazardous Materials , pp. 915-919, 2009.

[57] General Electric, "GE Lighting Product Catalog," 2013. [Online]. Available: http://genet.gelighting.com/LightProducts/Dispatcher?REQUEST=COMMERCIALSPECPAGE&PRODUCTCODE=10415&BreadCrumbValues=Lamps_Linear%20Fluorescent%5EFull%20Wattage&SearchFieldCode=null.

[58] C. Senior, A. Sarofim, T. Zeng, J. Heble and R. Mamani-Paco, "Gas-phase transformations of mercury in coal fired power plants," Fuel Processing Tech., vol. 63, pp. 197-213, 1999.

BIOGRAPHICAL SKETCH

Erica Wallace Gonzaga was born in Saint Paul, MN. Her family moved to her mother's home country of Brazil when she was 4 years old. Erica attended the American School of Brasilia, Brazil and moved to Fort Lauderdale, FL. after graduation in 2004. She started studying architecture at Broward College but after 2 years, decided to change her major to engineering. Erica was accepted to the University of Florida Biological Engineering program as a transfer student in the spring of 2009. She graduated with her bachelor's degree in December 2011 and spent the following semester working as a lab assistant for a PhD candidate in the department of Environmental Engineering. Erica was accepted as a Master of Engineering student in the Department of Environmental Engineering in the fall of 2012. One week before starting graduate school, Erica married her husband, Luiz Gonzaga, who is currently finishing is residency in Prosthodontics in the College of Dentistry at the University of Florida.